Quantitative neuroanatomy as a tool to understand cortical function

Part 1: methodological aspects

Almut Schüz

Max-Planck-Institut für
Biologische Kybernetik, Tübingen

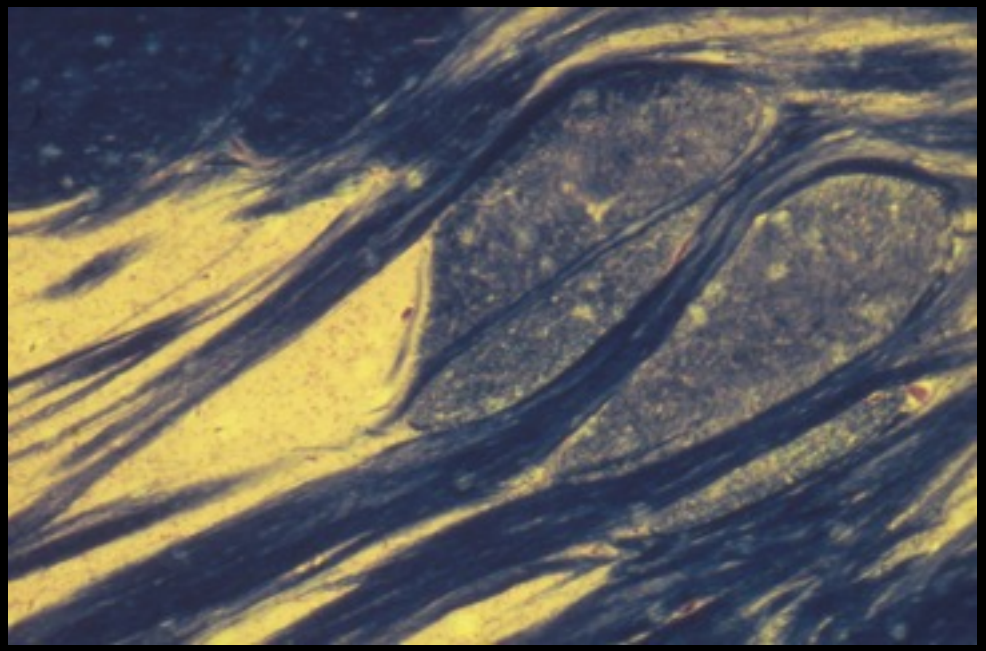

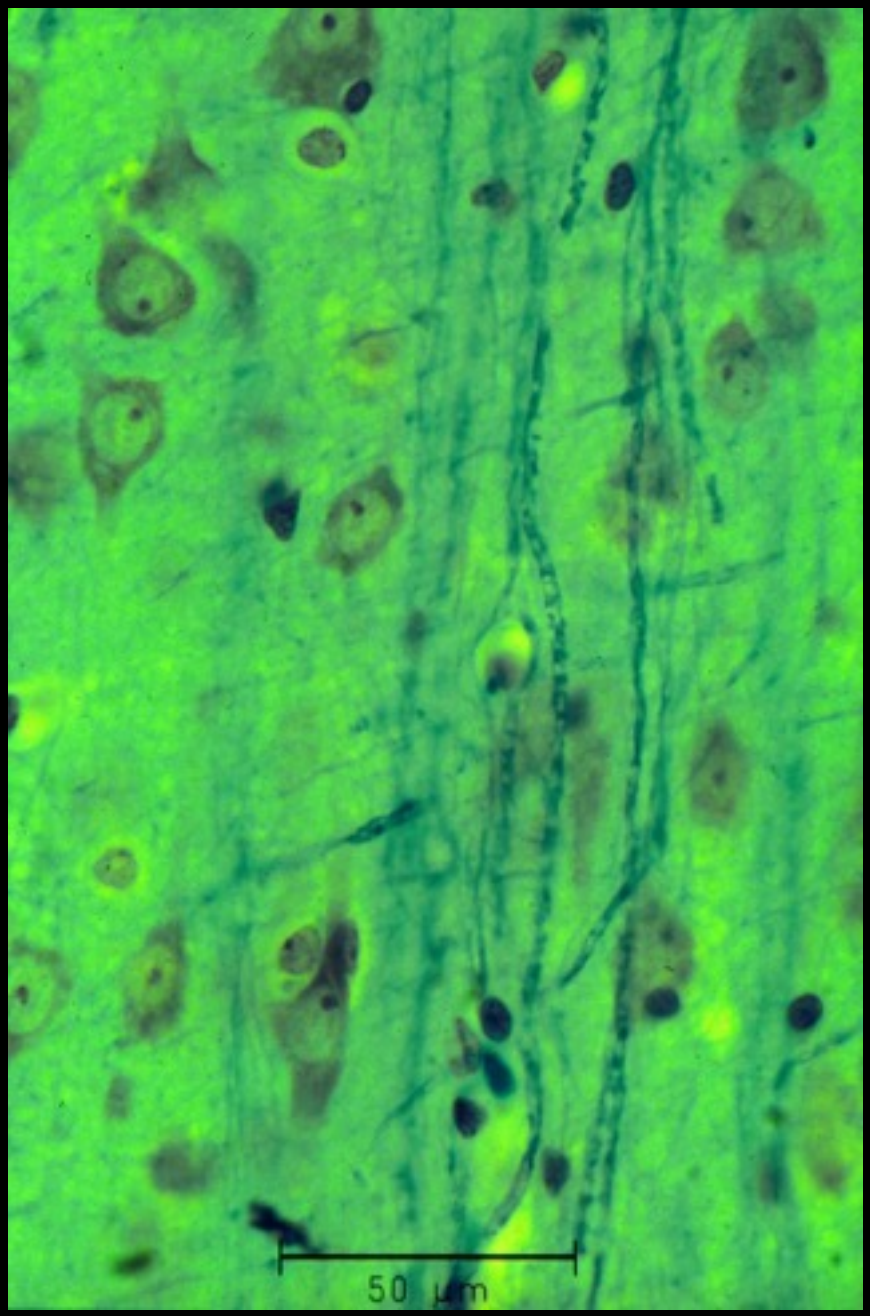

Cortico-cortical long-range connectivity: Anatomical data from mouse and monkey

Almut Schüz
Max Planck Institute for Biological Cybernetics, Tübingen, Germany

Sao Paulo, 26.11.2015

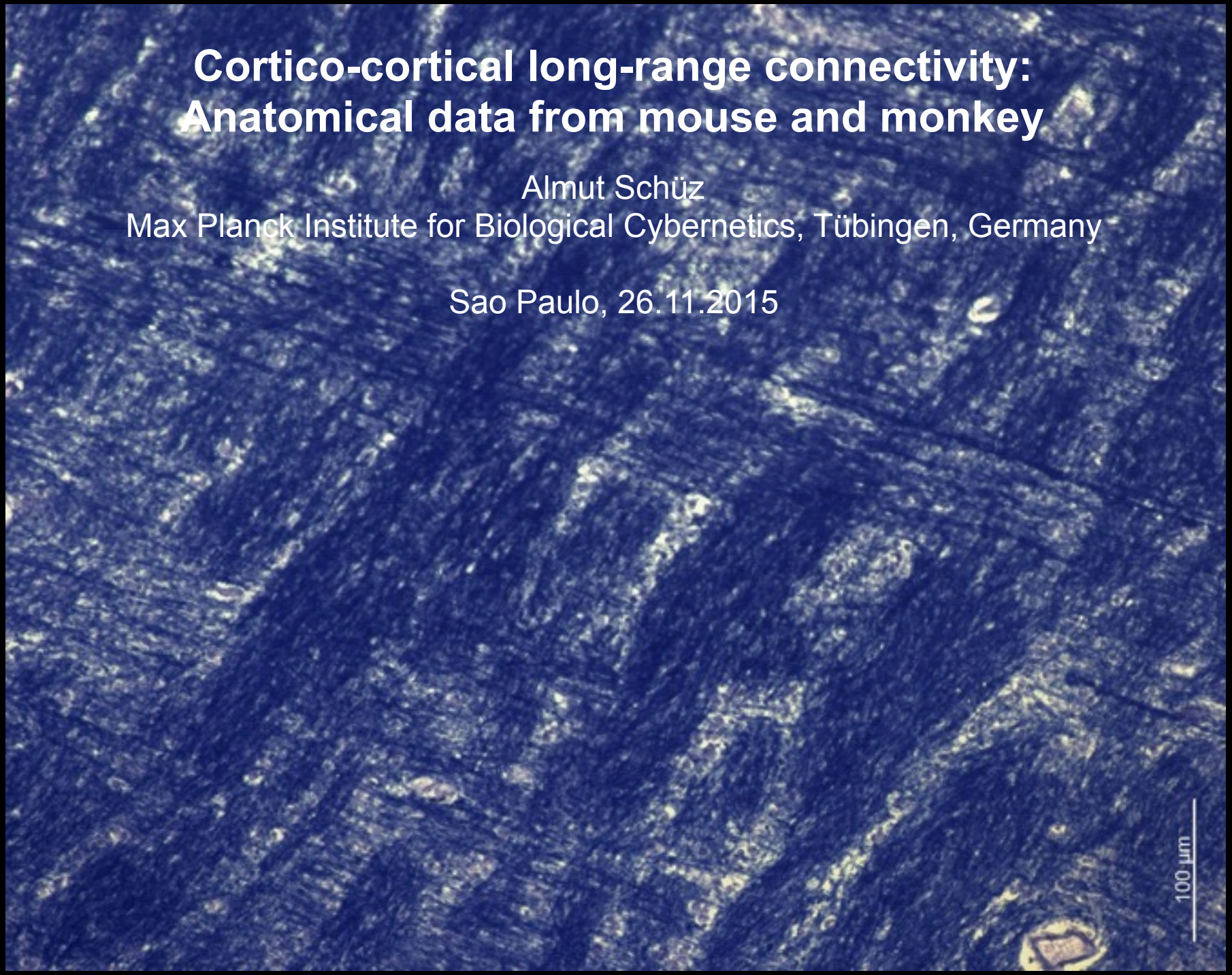

Quantitative neuroanatomy as a tool to understand cortical function

Part 1: methodological aspects

Almut Schüz

Max-Planck-Institut für
Biologische Kybernetik, Tübingen

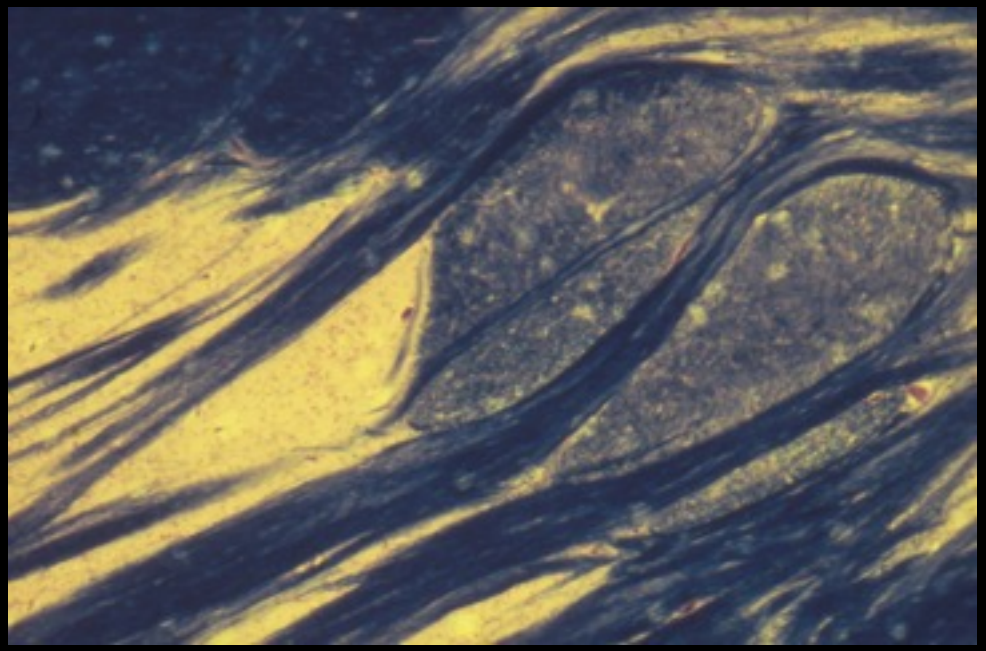

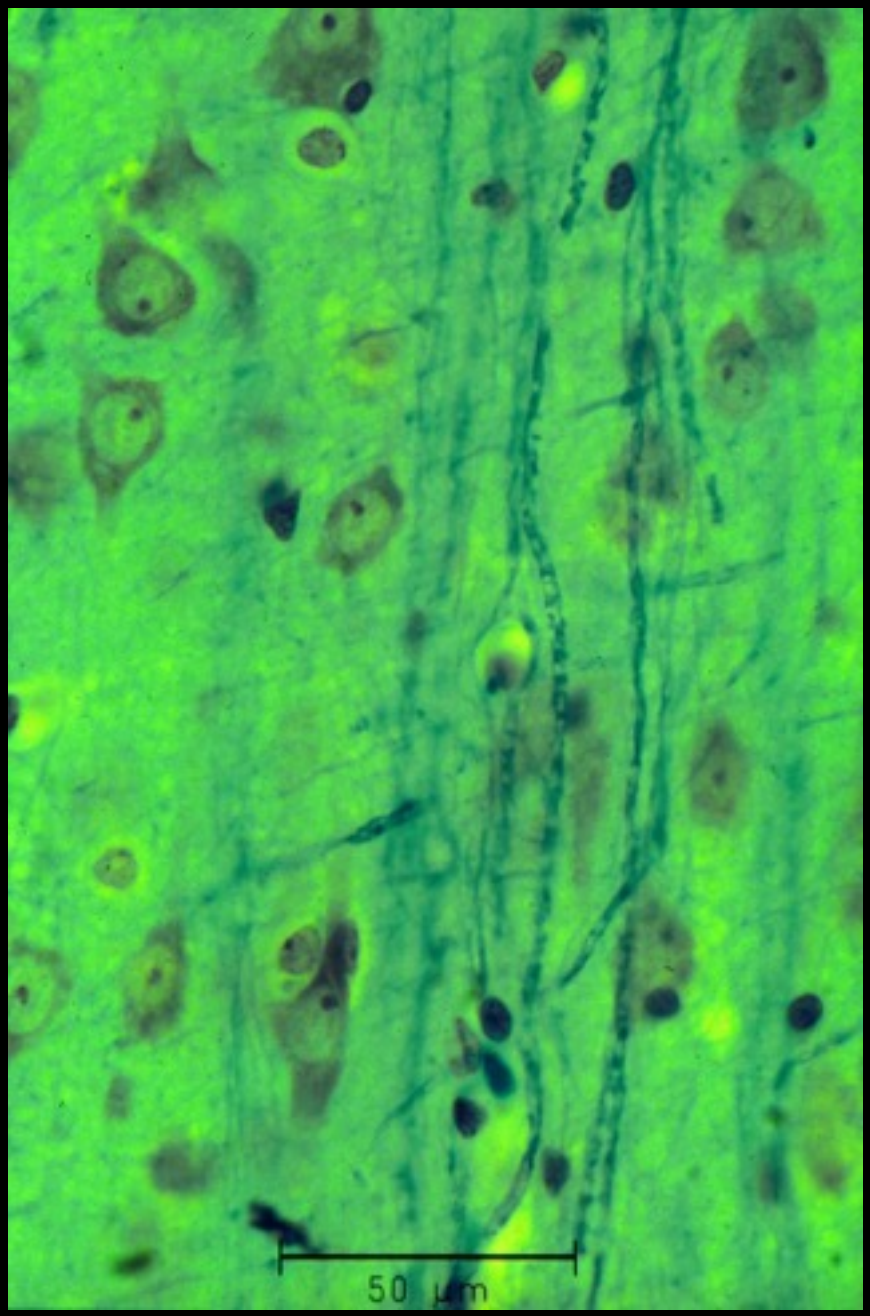

Valentino Braitenberg , 1926 - 2011

Sistema visivo della mosca

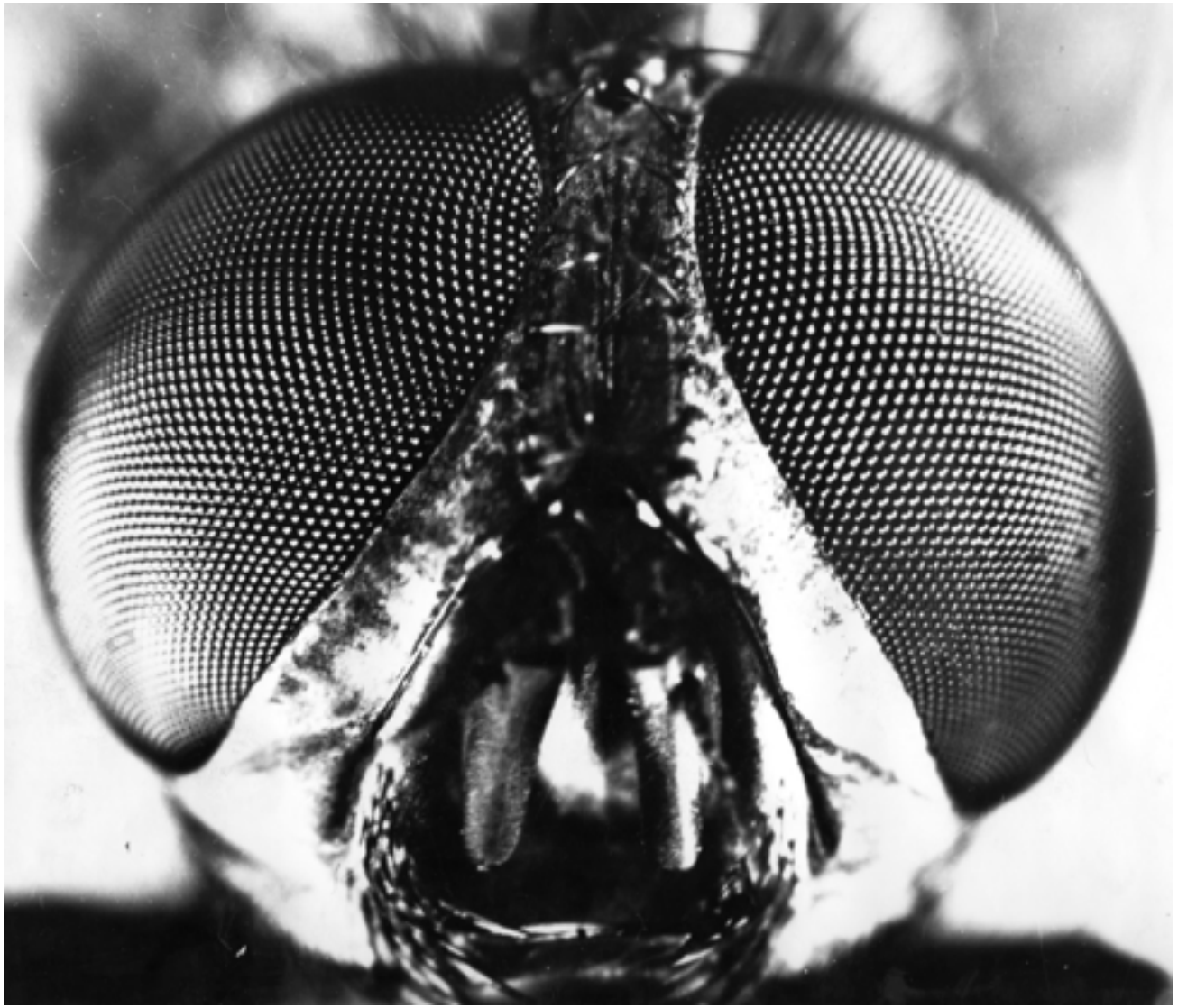

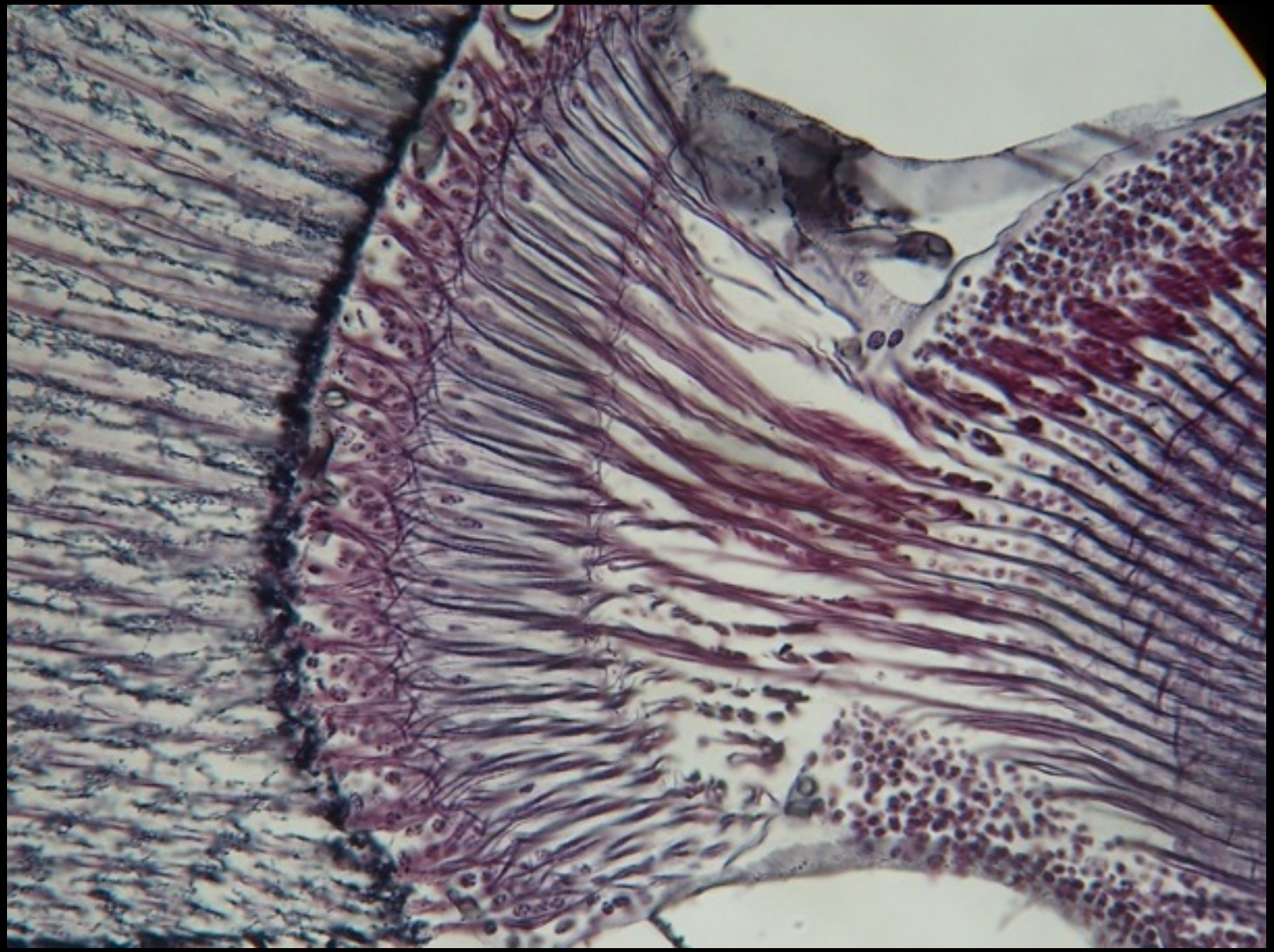

Horizontal section through the fly visual system. From: Valentino Braitenberg

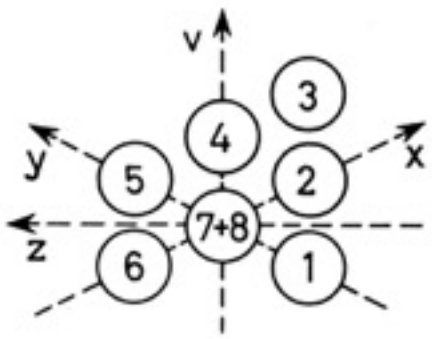

Abb. 6. Die Retinula, d. h. die Anordnung der Enden der sieben Lichtleiter in der Brennebene (Abbildungsebene) eines Ommatidiums (f in Abb. 5). Das Schema entspricht der Anordnung in der oberen Hälfte des rechten Auges, von außen gesehen. v und z markieren die Richtung nach oben bzw. nach hinten im Gesichtsfeld, x und y sind die beiden schrägen Richtungen der hexagonalen Anordnung der Ommatidien im Komplexauge der Fliege

From: Valentino Braitenberg, Gehirngespinste (1973)

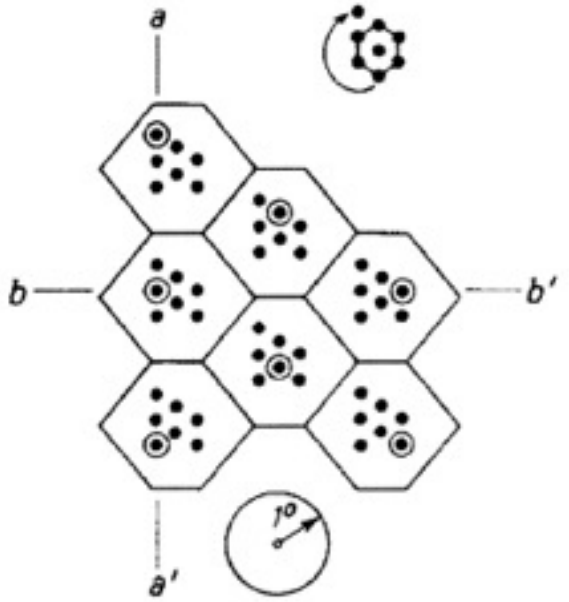

From Kuno Kirschfeld (1967)

Fibres crossings between the ommatidia and the first visual ganglion.
From V.Braitenberg

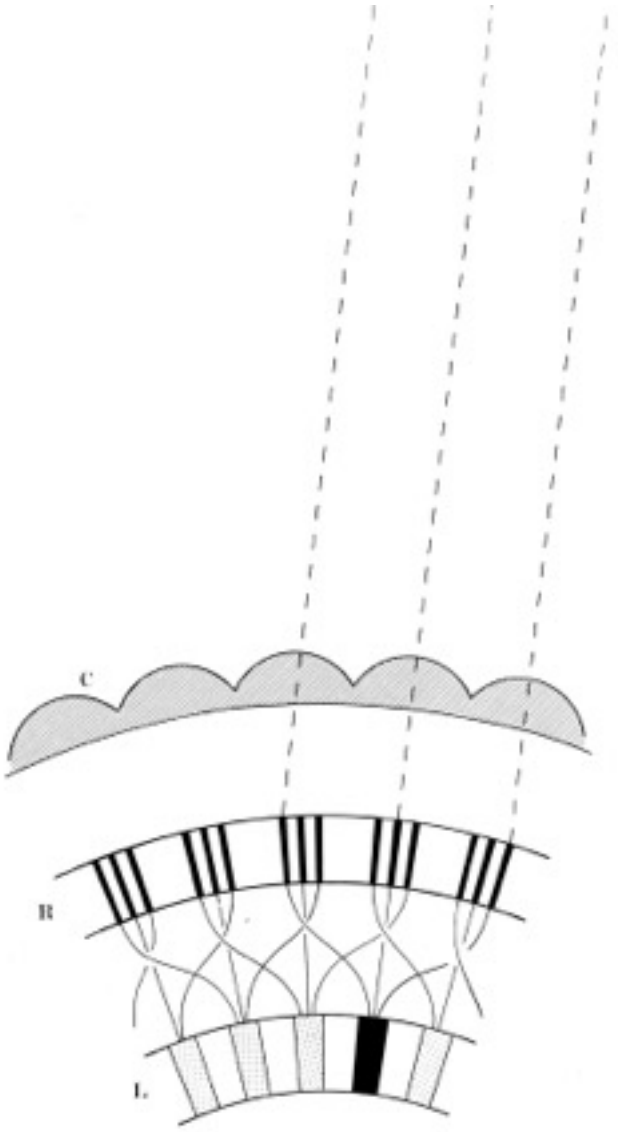

From Valentino Braitenberg,
Gehirngespinste (1973)

Specificity of synapses

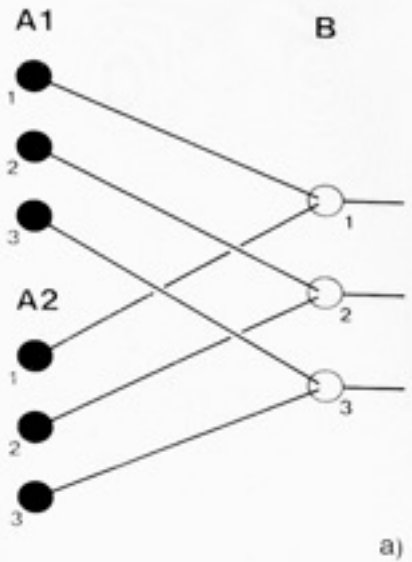

Specificity of synapses

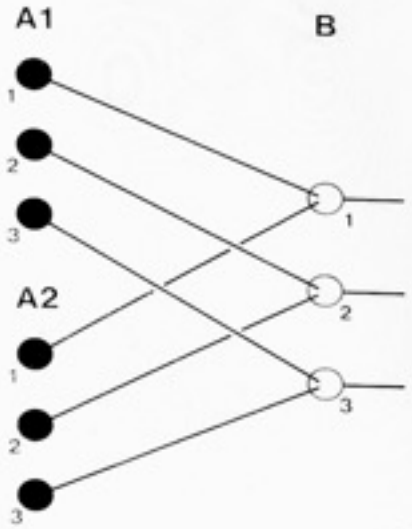

Specificity of cell types

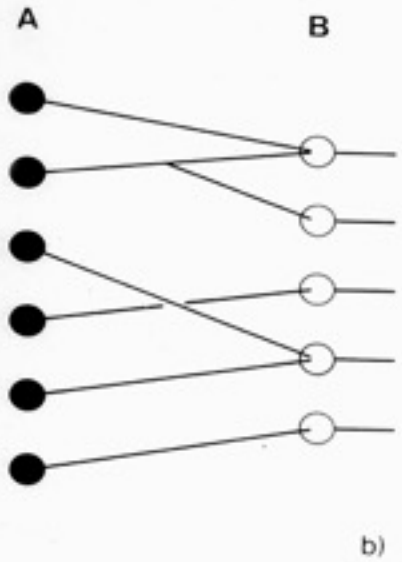

Specificity of synapses

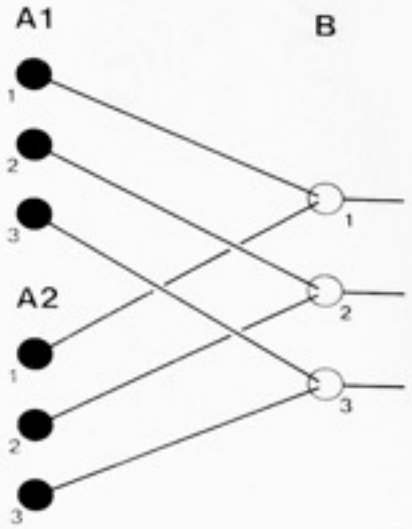

Specificity of cell types

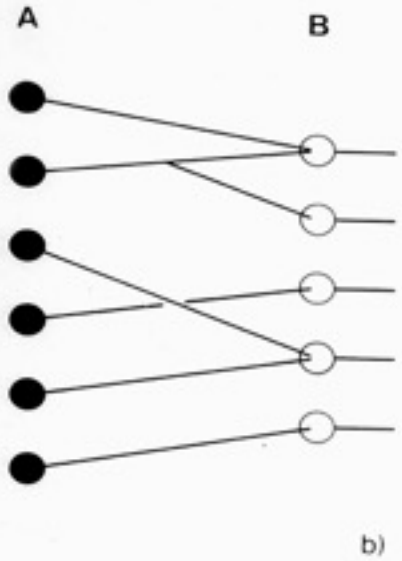

Statistical connectivity

Cortical Functions

Learning
Thinking
Perception (acoustic, visual, tactile, olfactory)
Recognition
Voluntary movements
Language
Categorisation
Calculating
Composing music …

Variety of functions –

Relative homogeneity of structure

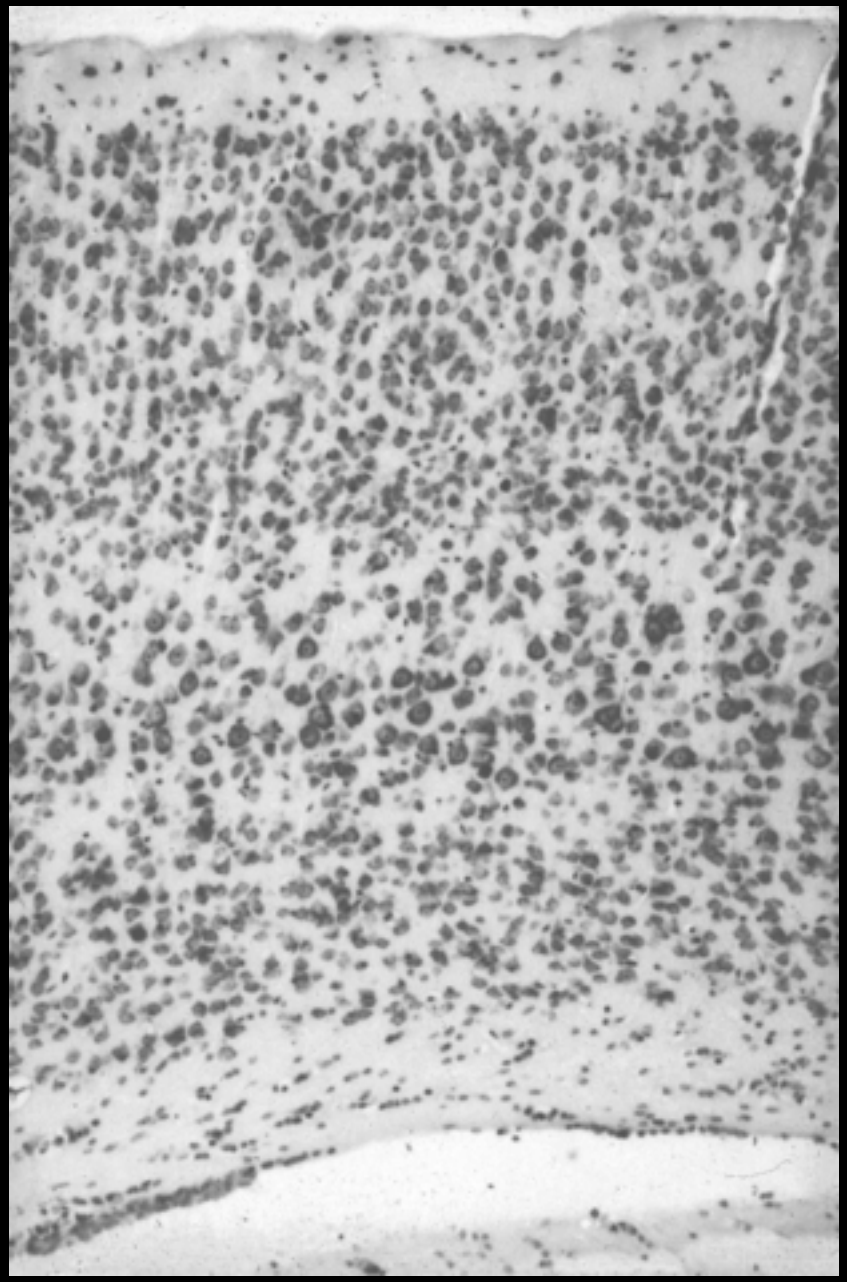

0.1 mm

Nissl-stain,
visual cortex, mouse
From:
Braitenberg and Schüz (1991/98)

Golgi-stain,
Cat cortex,
Pyramidal cells

somatosensory

acoustic

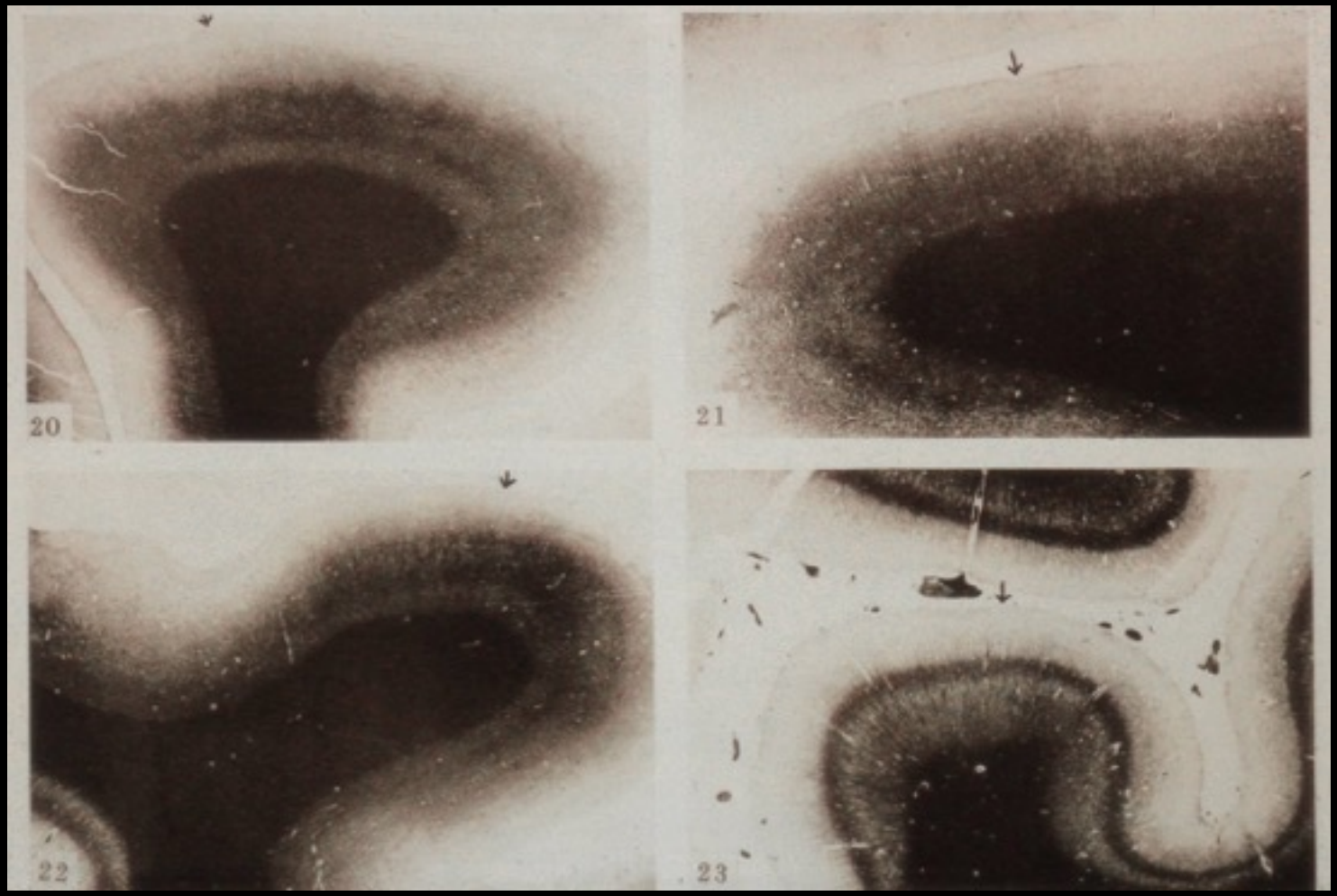

V2

V1

From: Valentino Braitenberg

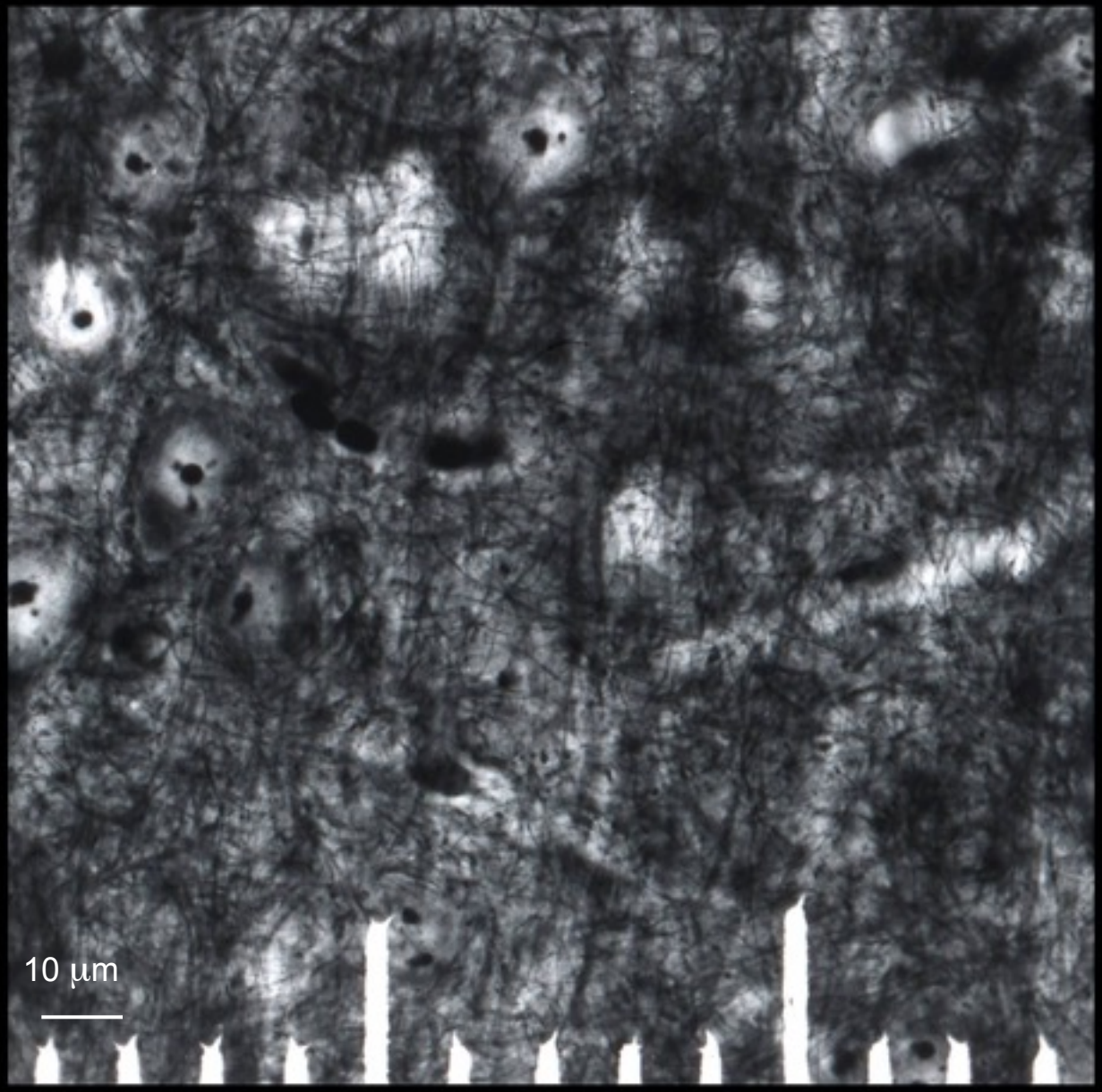

From: Valentino Braitenberg (1981)

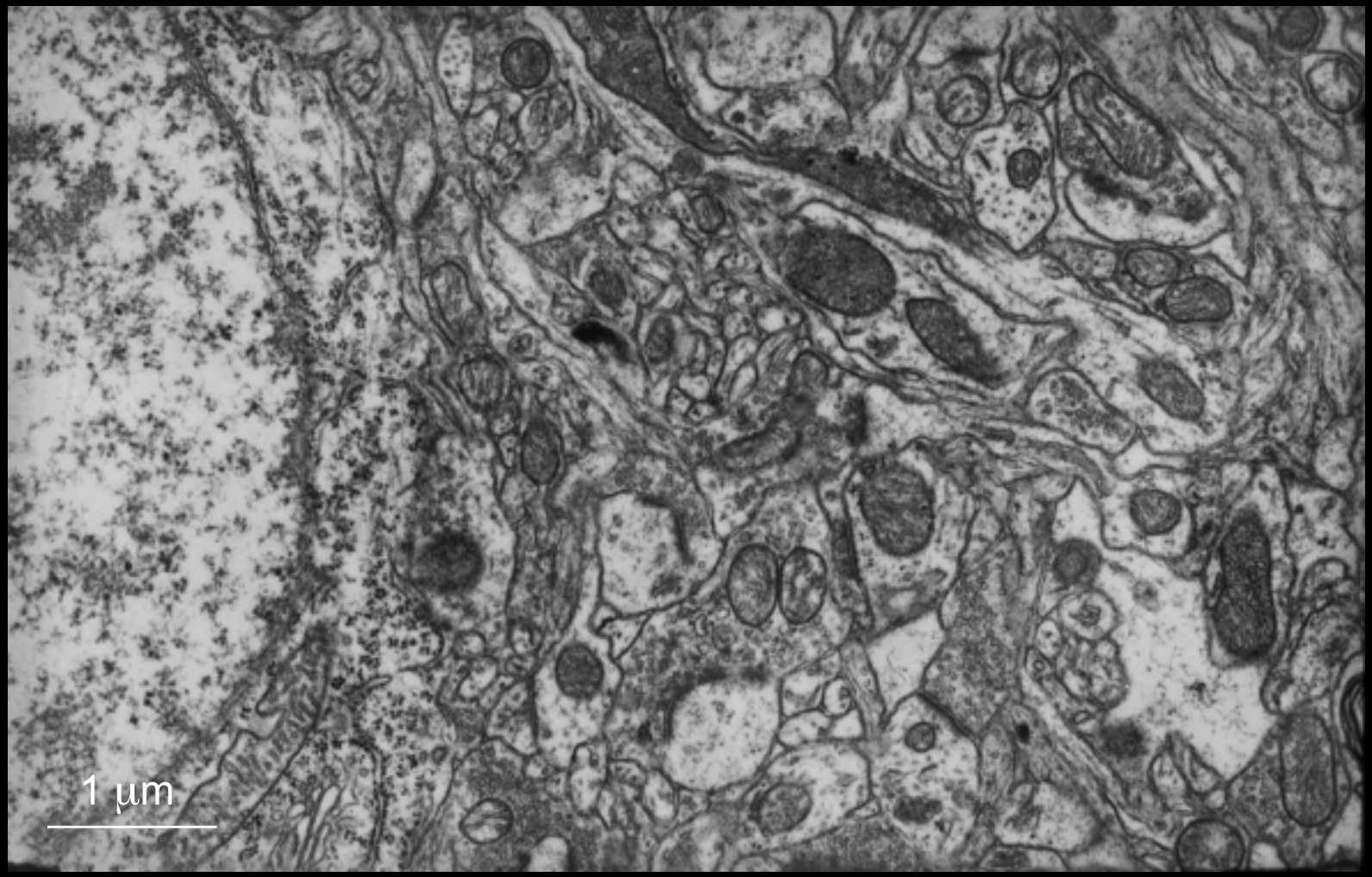

Electron microscopy, cortex, Osmium stain

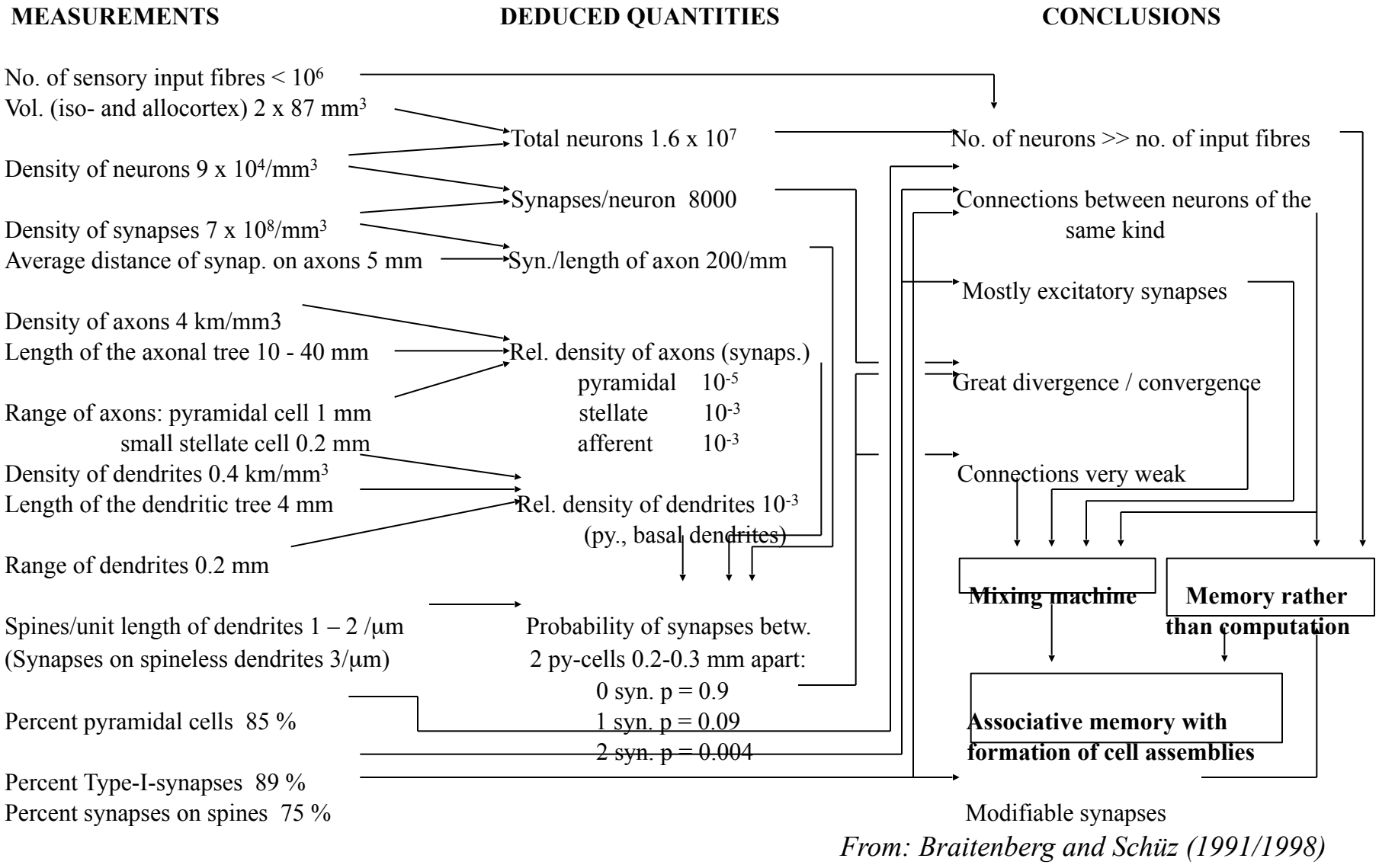

From: Braitenberg and Schüz (1991/1998)

Methodological problems in quantitative neuroanatomy

- Completeness of stain

- Unambiguous recognition of structures

- Shrinkage

- transformation of number per area into number per volume

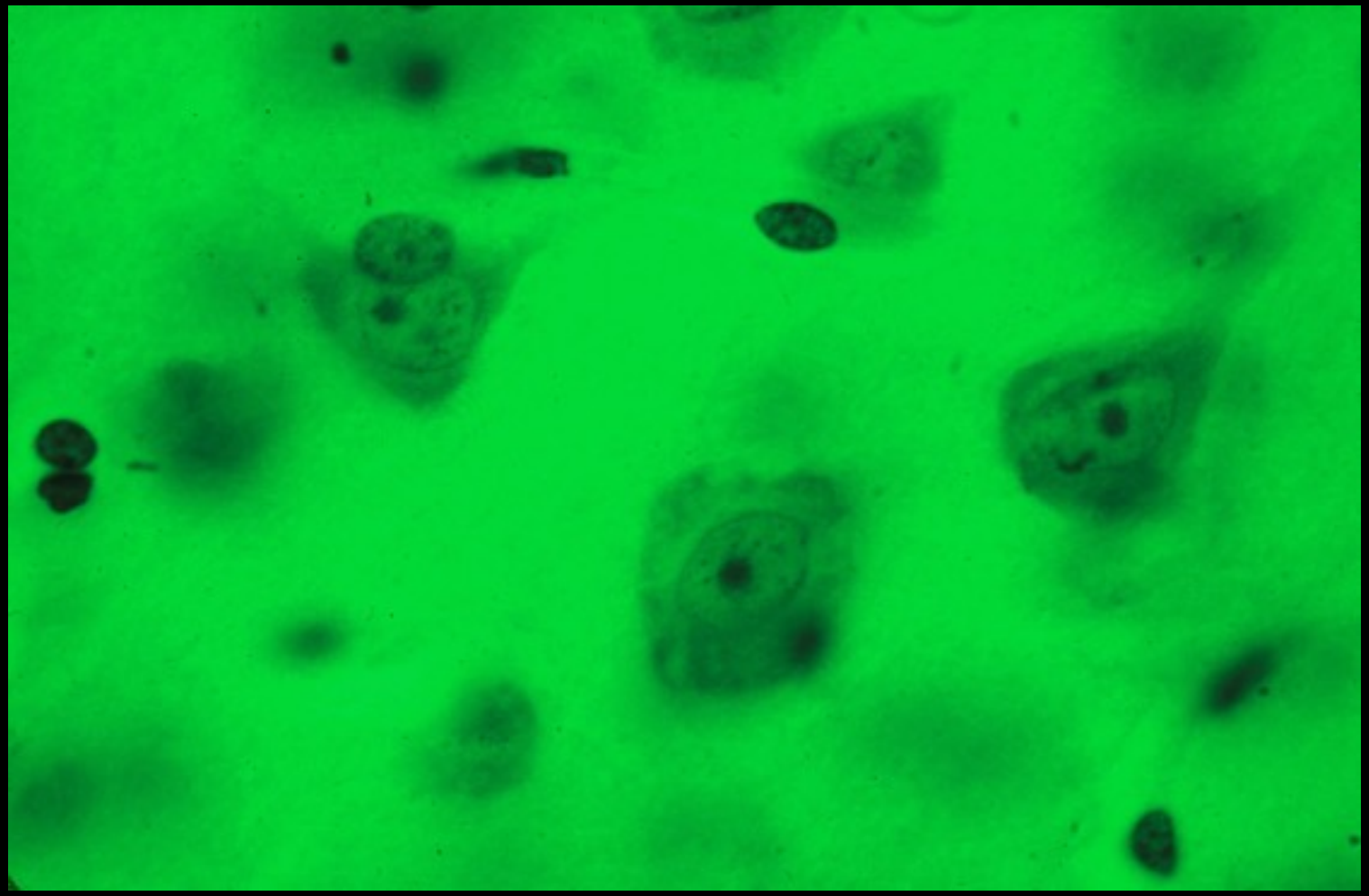

Nissl stain human cortex, layer 5,
From Schüz (2008), Scholarpedia, 3(3):3158.

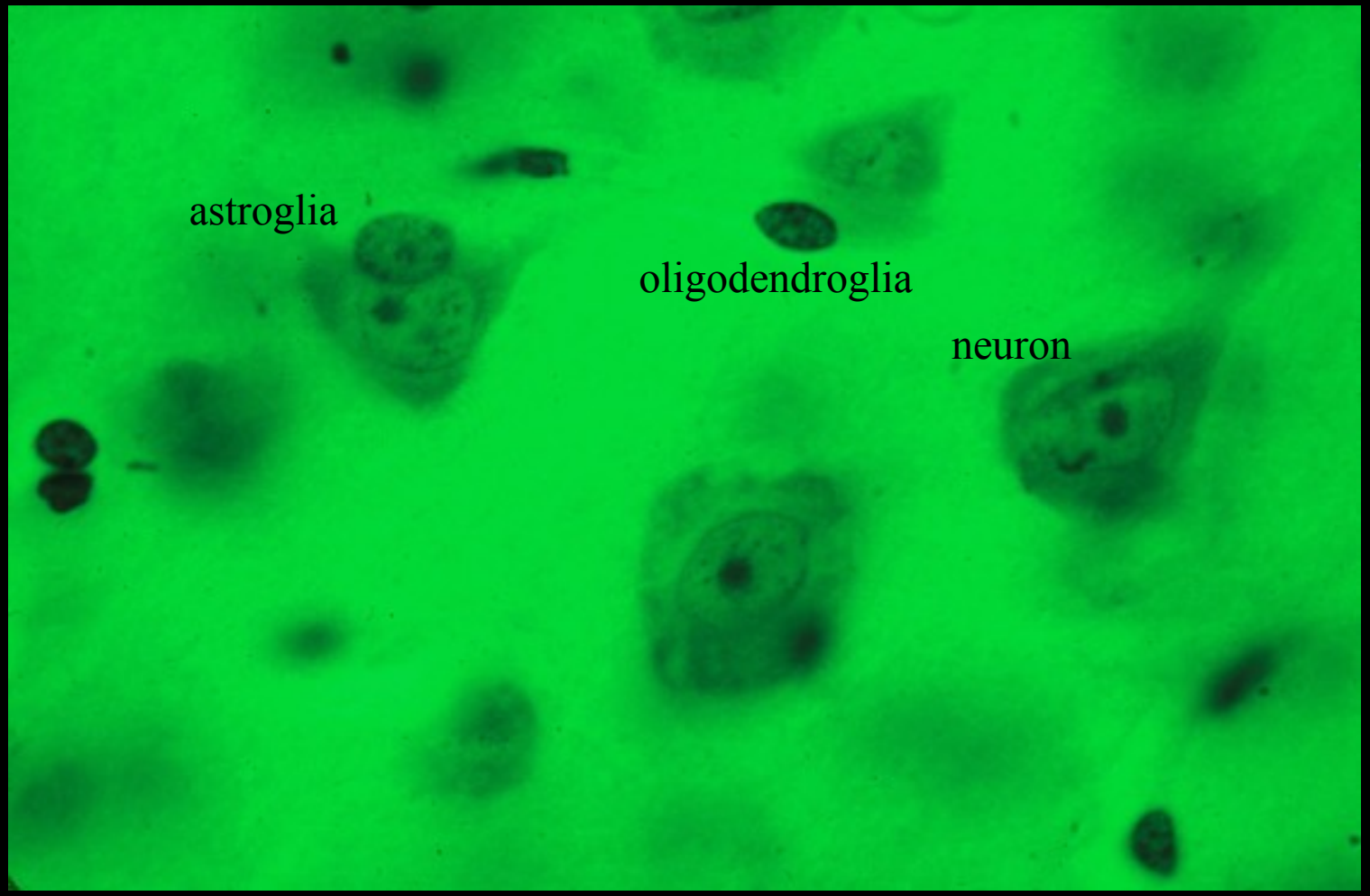

Nissl stain human cortex, layer 5,
From Schüz (2008), Scholarpedia, 3(3):3158.

Laver IV
Mouse
cortex

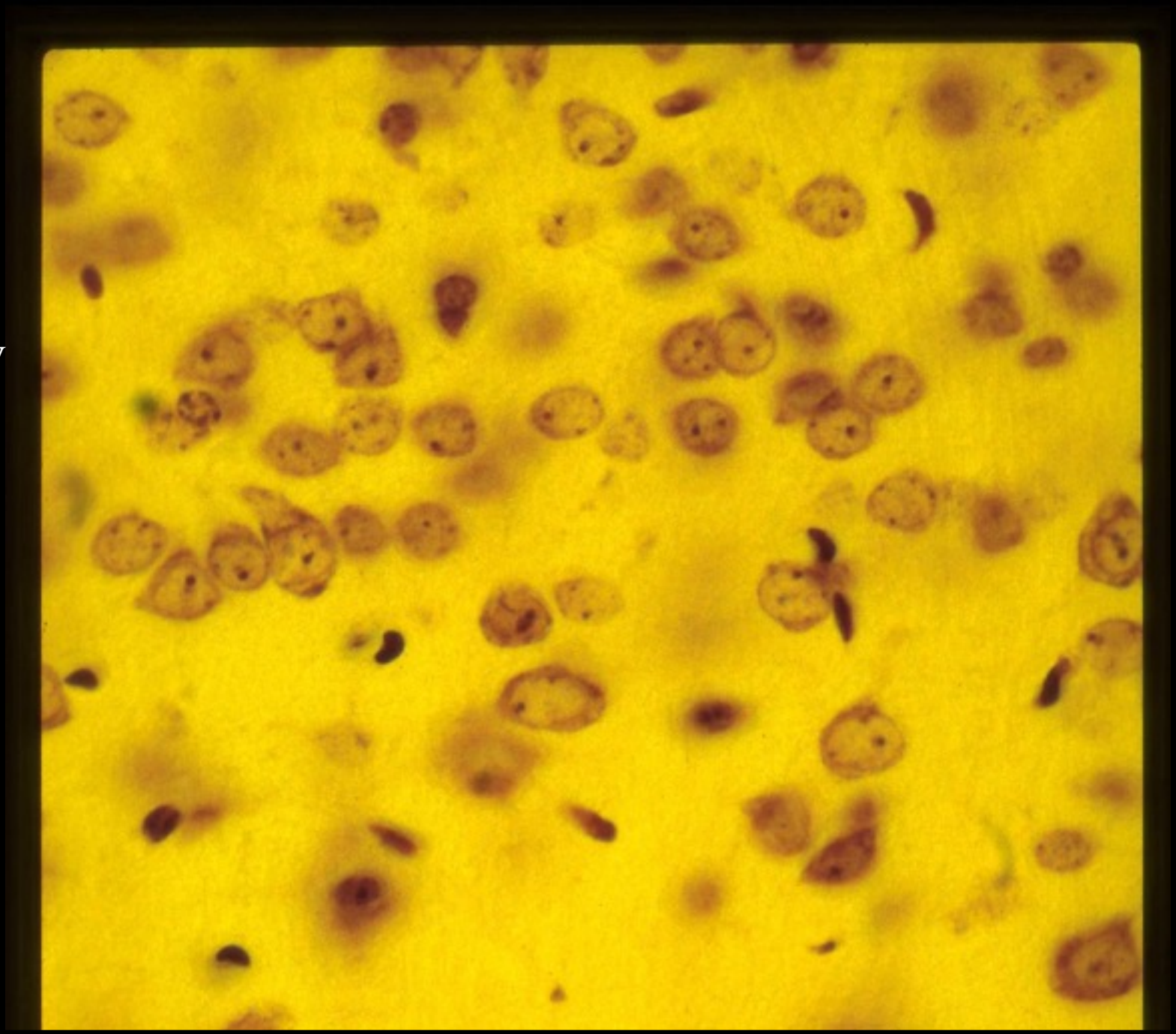

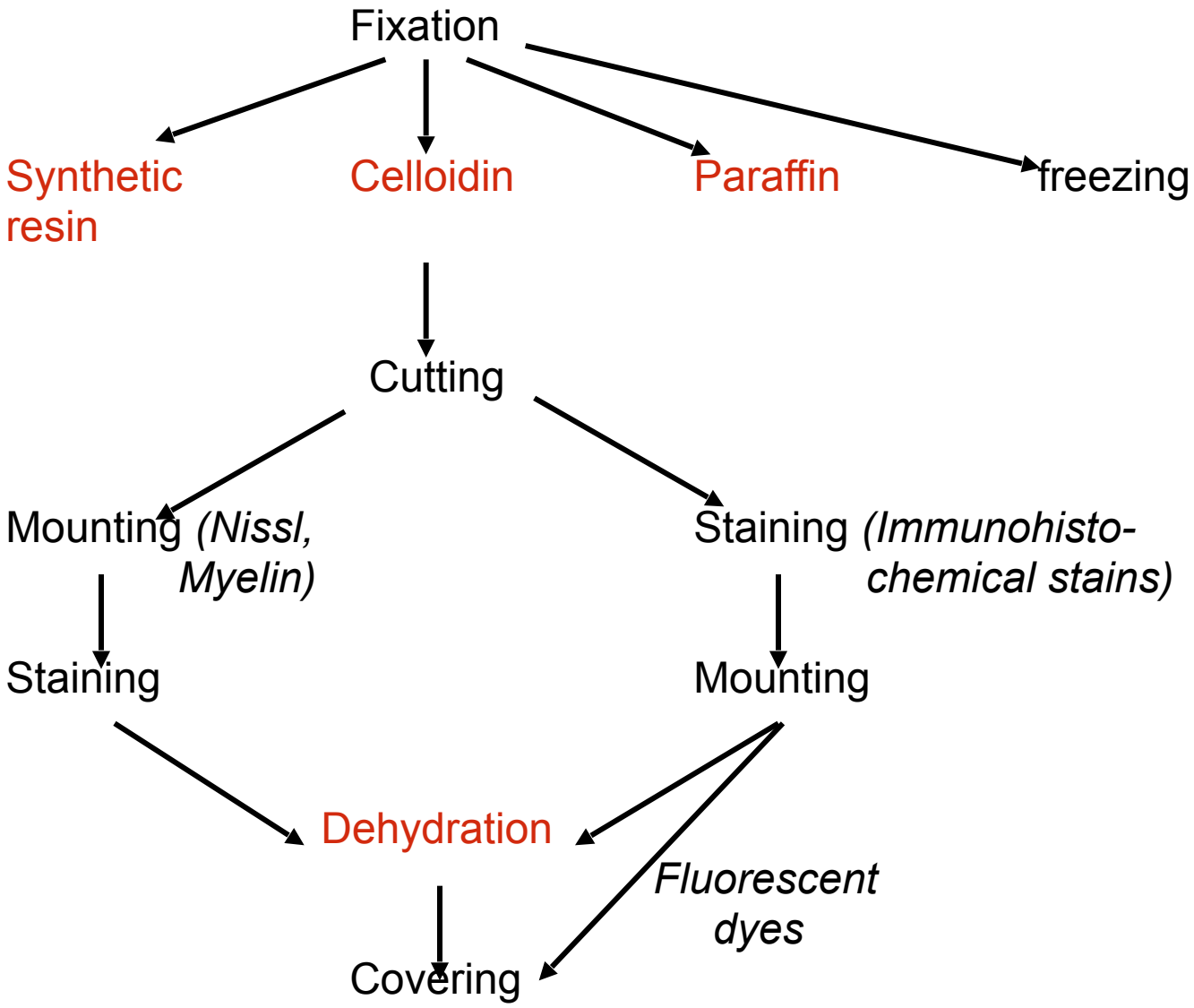
Fixation
Synthetic resin
Celloidin
Paraffin
freezing
Cutting
Mounting (Nissl, Myelin)
Staining (Immunohisto-chemical stains)
Staining
Mounting
Dehydration
Fluorescent dyes
Covering

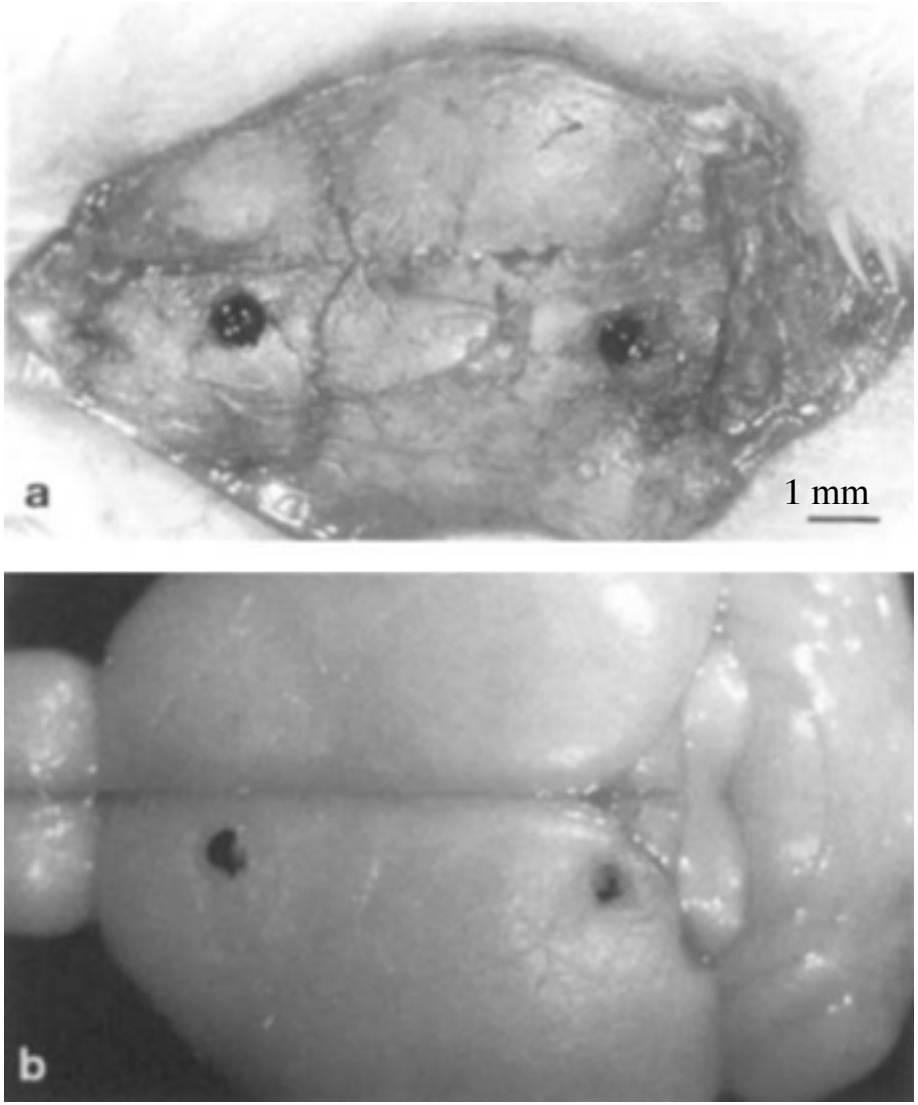

From: Schüz and Palm (1989)

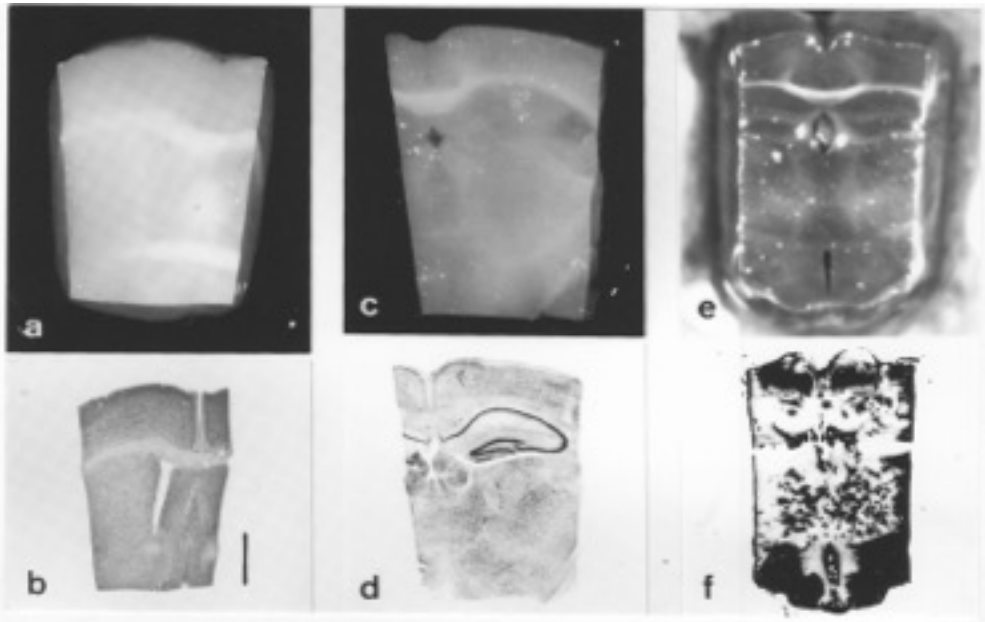

Abb. 15: Schrumpfung des Gewebes bei verschiedenen lichtmikroskopischen Methoden. Maßstab: 1 mm. Oben die fixierten Scheiben, a) und c) mit 3,7% Formalaldehyd, e) mit Glutaraldehyd und Kaliumbichromat. Darunter jeweils ein Schnitt von der darüberliegenden Scheibe. b) Nisslfärbung am Paraffinschnitt, c) Nisslfärbung am Gefrierschnitt, f) Golgi-Färbung und Celloidineinbettung.

From: Schüz and Palm (1989)

Method	Linear schrinkage	Volume shrinkage
Nissl stain after paraffin embedding	≈ 0.75 (0.67 – 0.81)	to 42 %
Nissl stain on frozen sections	≈ 0.88	to 68 %
Golgi stain and celloidin embedding	≈ 0.89	to 70 %
Electron microscopic material (osmium)	swelling and shrinkage compensate each other	no change in volume

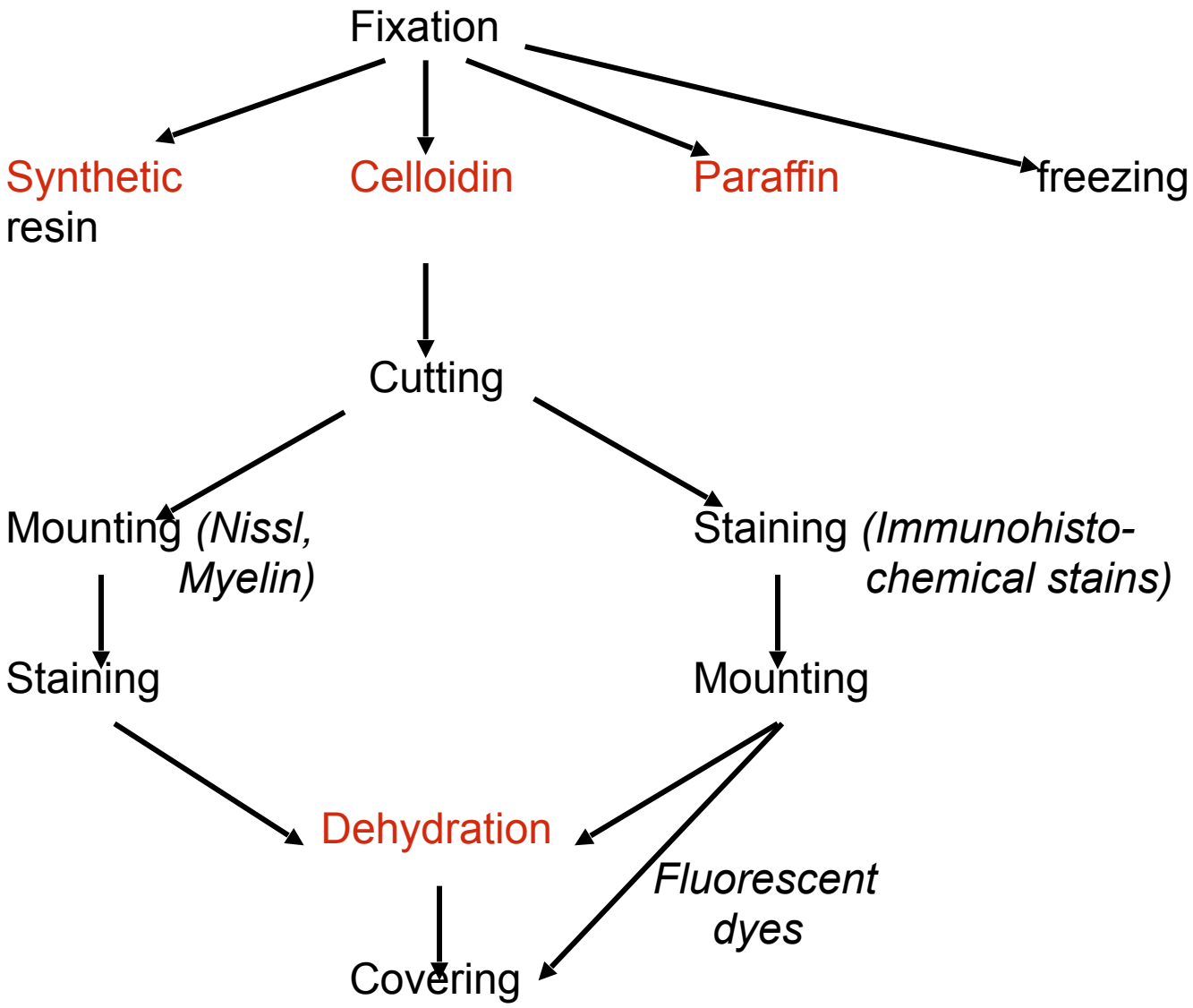
Fixation
Synthetic resin
Celloidin
Paraffin
freezing
Cutting
Mounting (Nissl, Myelin)
Staining (Immunohisto-chemical stains)
Staining
Mounting
Dehydration
Fluorescent dyes
Covering

Transformation of number per area to number per volume:

Stereology

Transformation of number per area to number per volume:

Stereology

-Counting cell bodies

-Counting synapses

-Length of dendrites or axons per neuron

-Density of axons per mm^3

-Density of spines per dendritic length

-Density of synapses along dendrites

-Density of synapses along axons

-Probability of connections between neurons

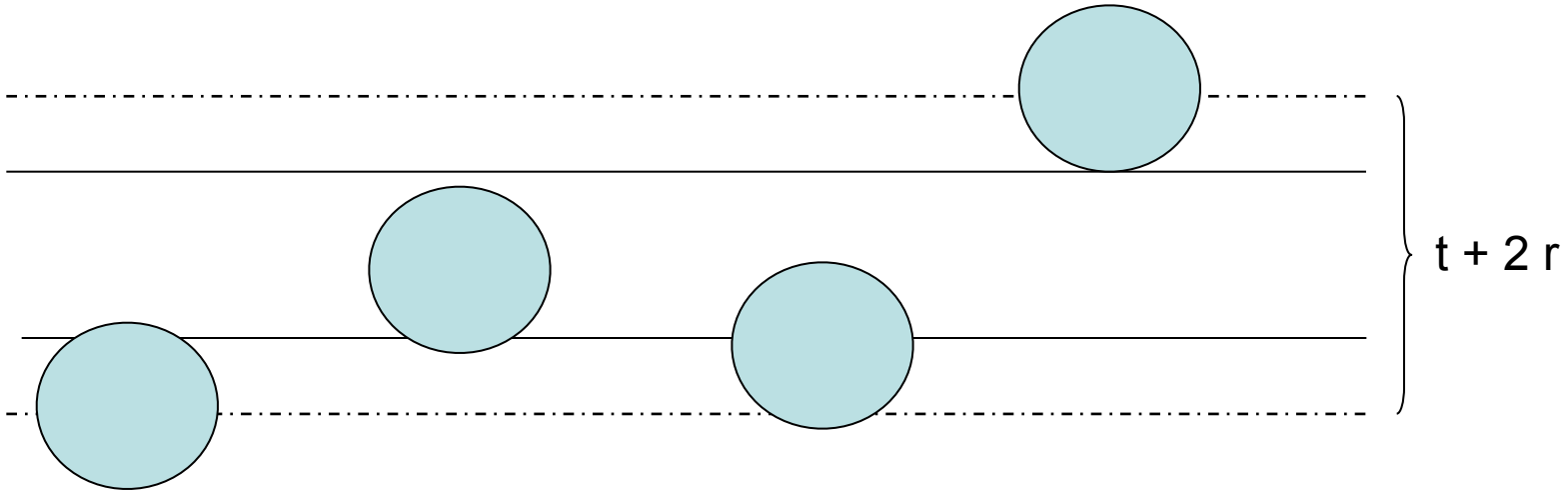

$t \sim 10 - 30\ \mu m$

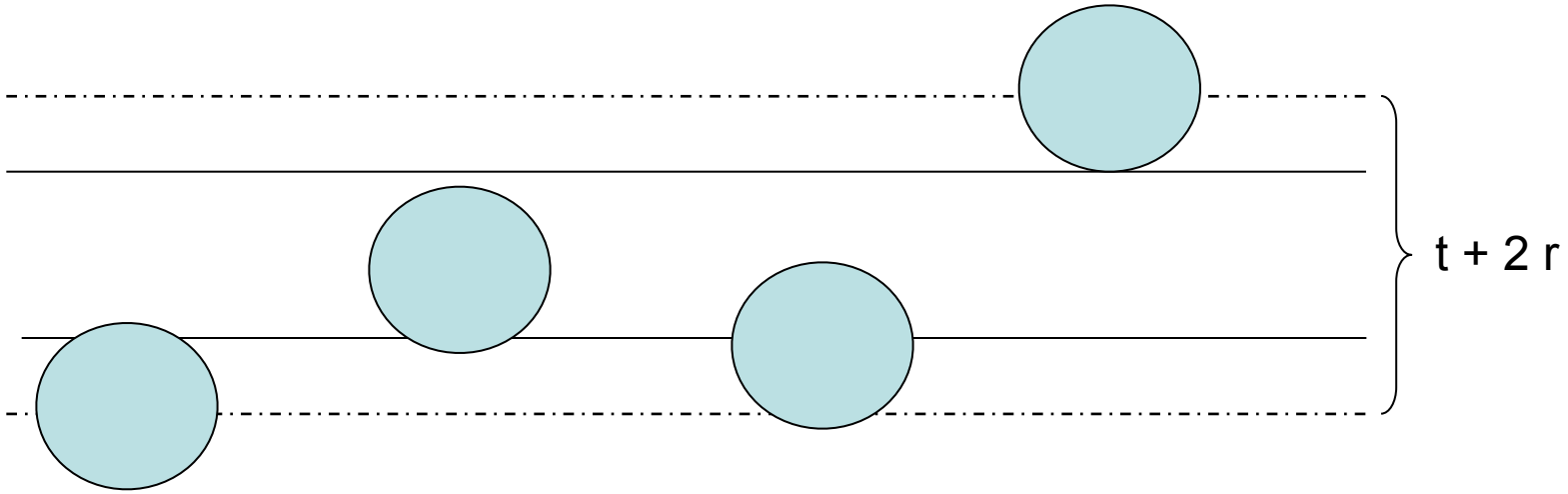

$t \sim 10 - 30\ \mu m$

$$N / V = \frac{N_{counted}}{Area \times (t + 2 \times radius)}$$

(Abercrombie, 1946)

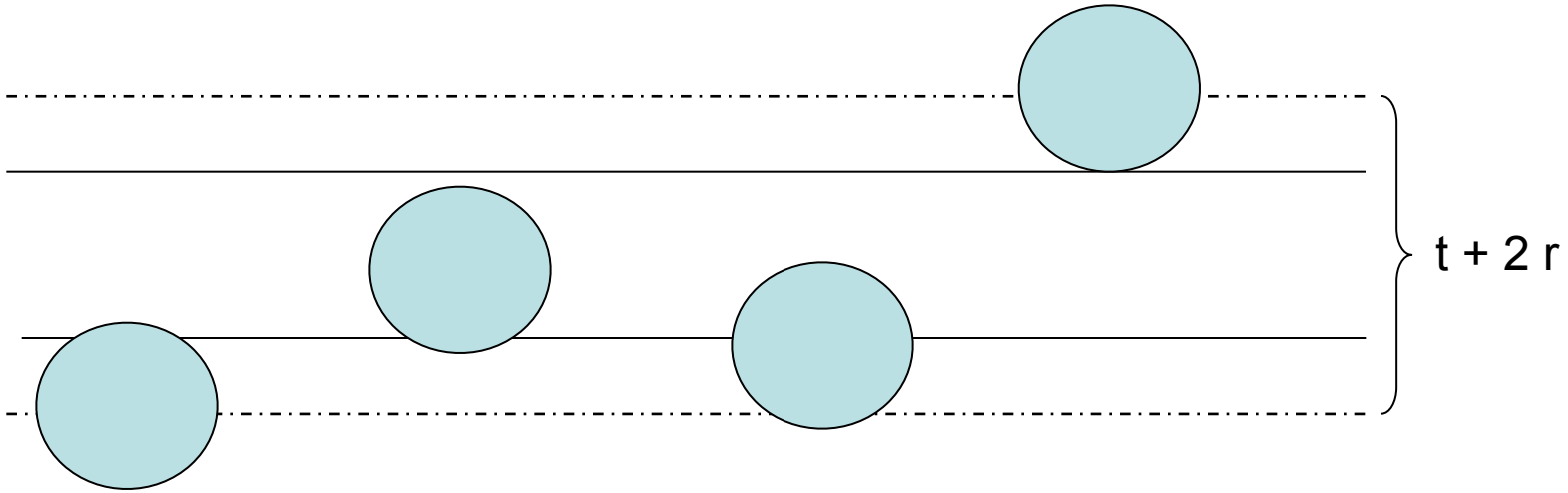

Alternative approaches:

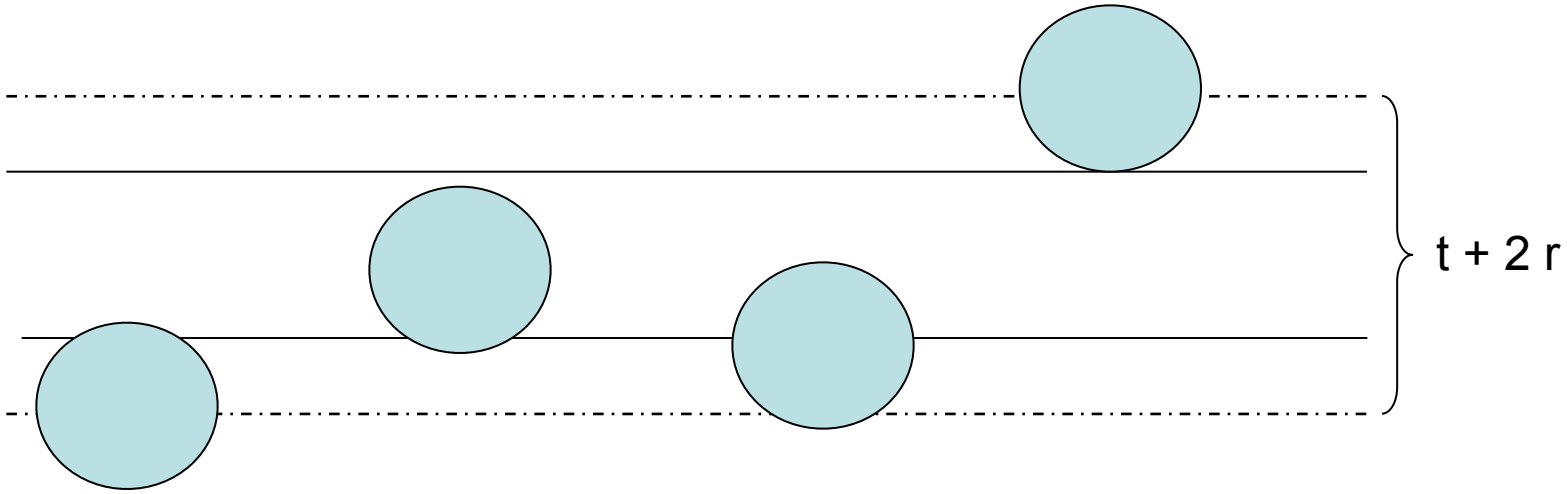

Alternative approaches:

determining the center of each neuron by focussing

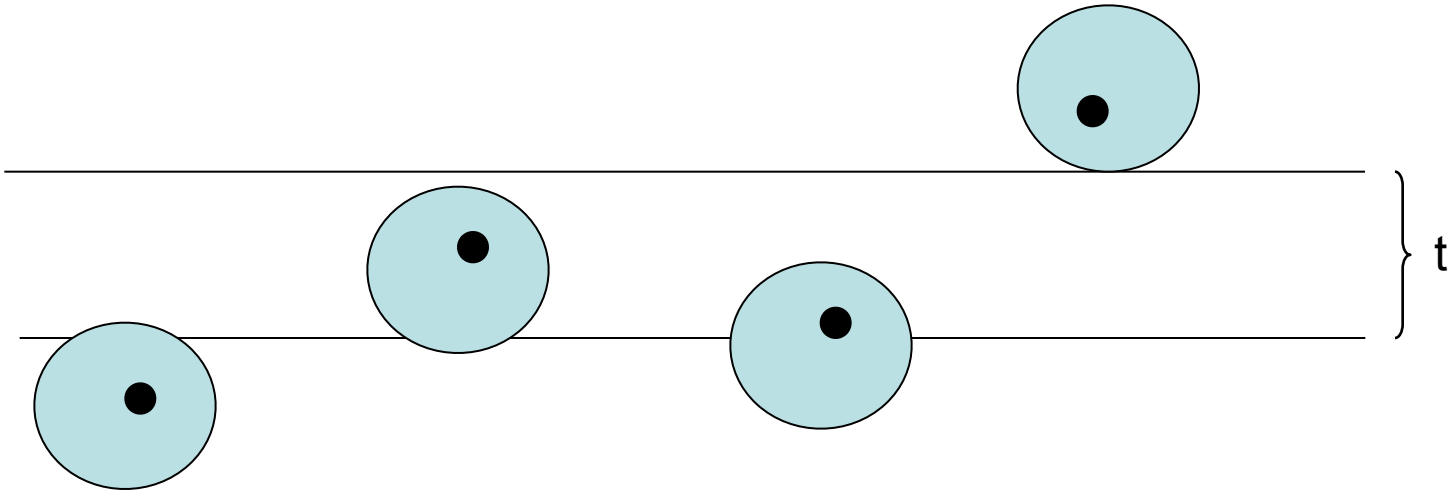

Alternative approaches:

determining the center of each neuron by focussing

counting nucleoli

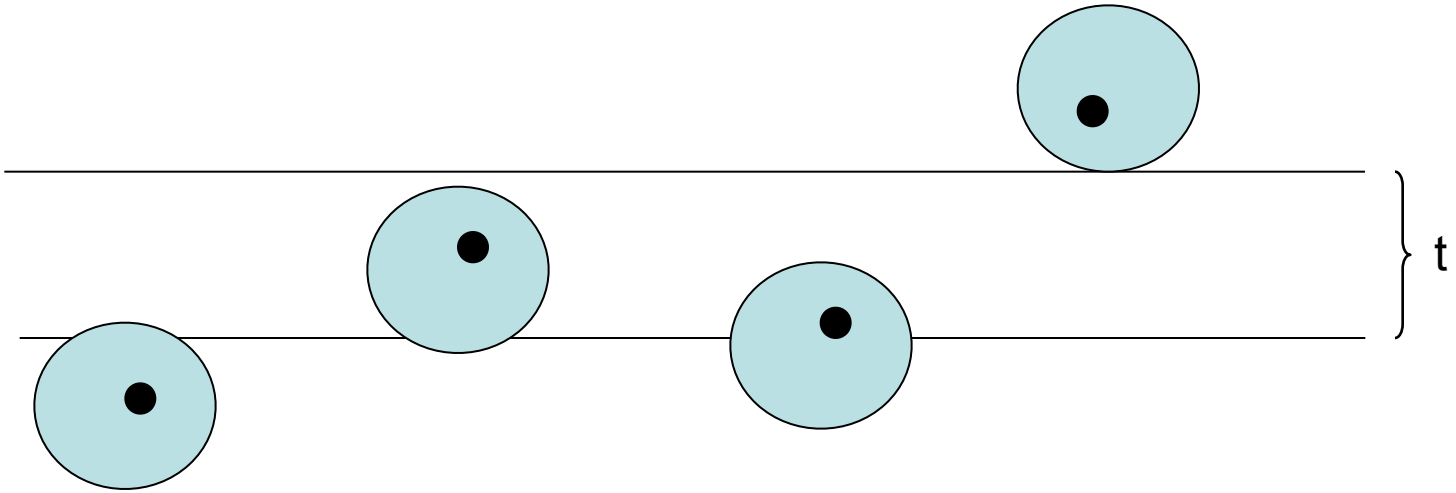

Alternative approaches:

determining the center of each neuron by focussing

counting nucleoli

Bok‘s method (1959): using 2 alternating section thicknesses

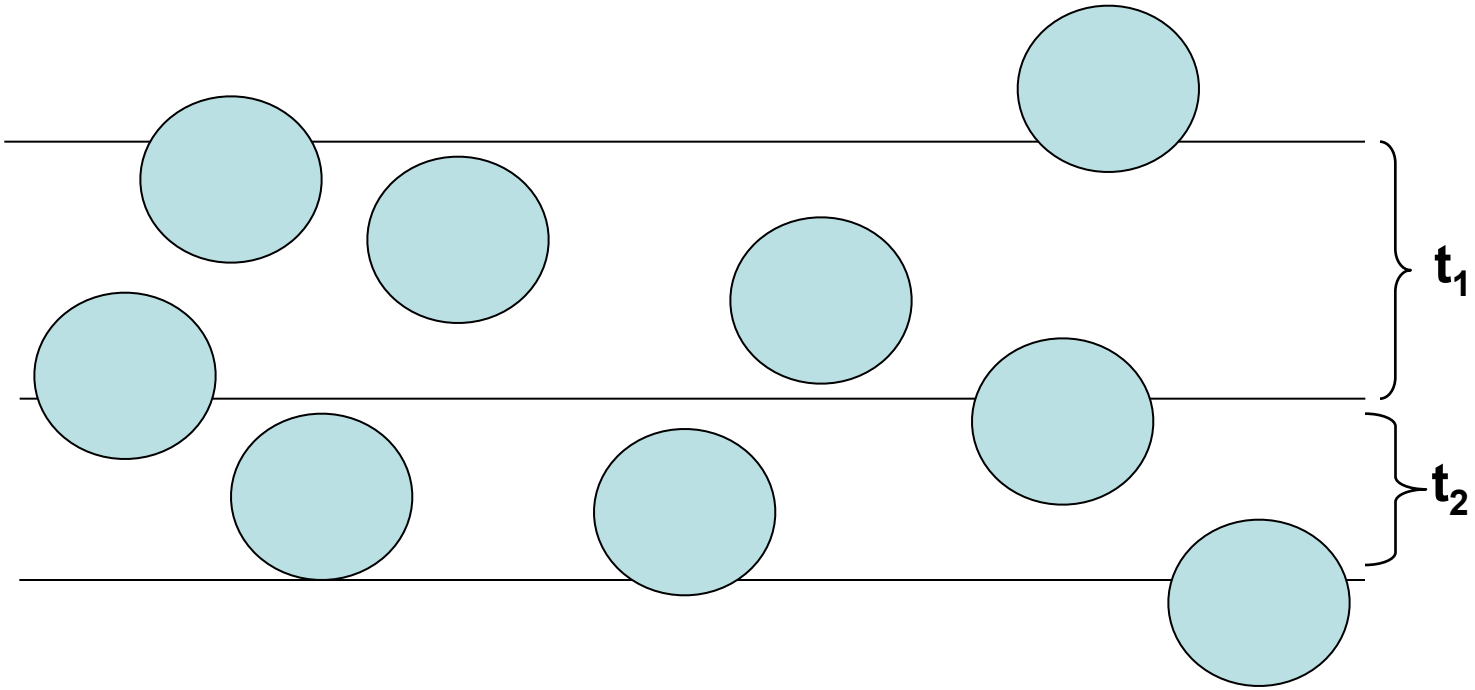
t_1
t_2

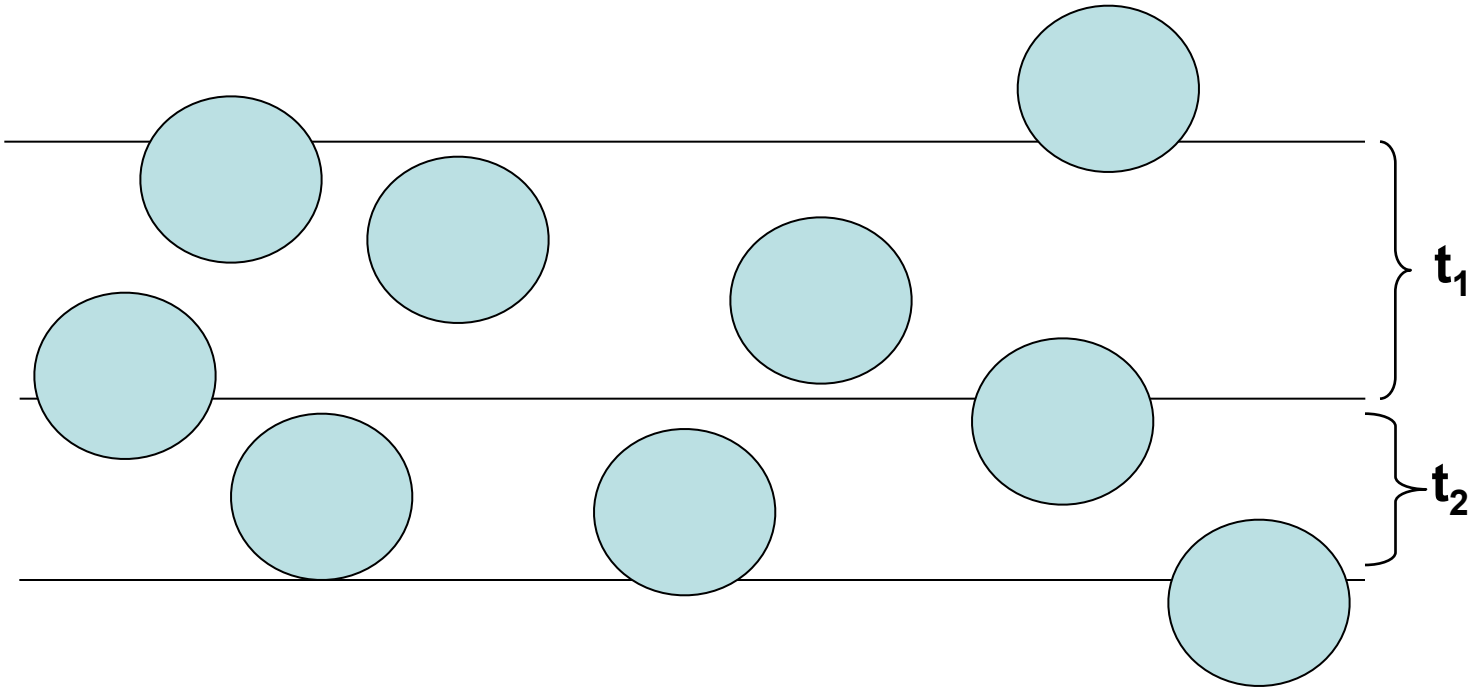

$$N / V = \frac{N_1 - N_2}{\text{Area} \times (t_1 - t_2)}$$

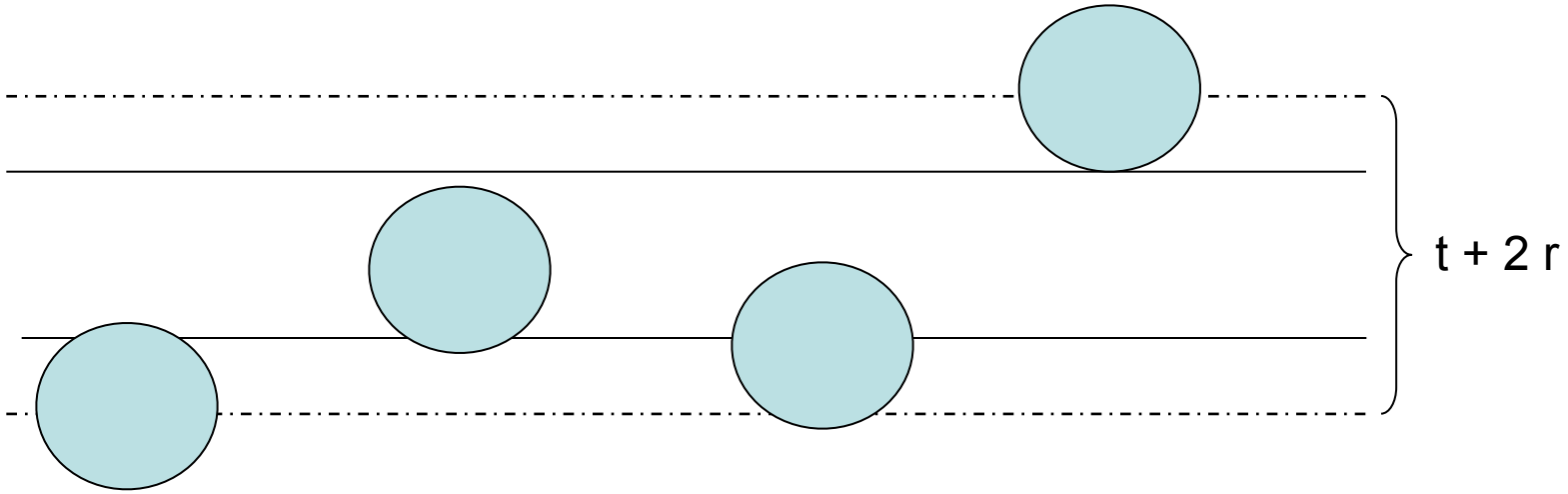

$$N / V = \frac{N_{counted}}{\text{Area} \times (t + 2 \times \text{radius})}$$

(Abercrombie)

Günther Palm (now chair for neuroinformatic, University of Ulm)

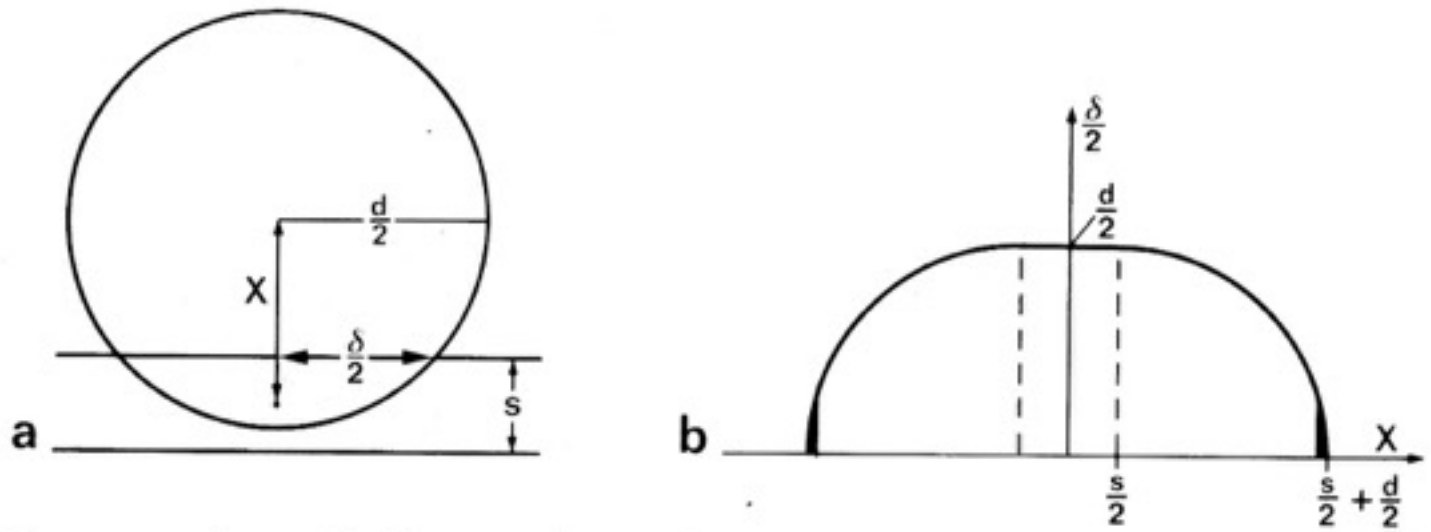

Fig. 7. **a** A sphere with diameter d is partly contained in a slice of thickness s. x is the distance between the center of the sphere and the middle layer of the slice. δ is the diameter of the part contained in the slice. **b** Dependence of δ on x. This is the distribution of apparent diameters δ if all the positions of particles of uniform size relative to a histological section occur with equal probability.

$$\bar{\delta} = \frac{ds + \pi d^2/4}{s + d}$$

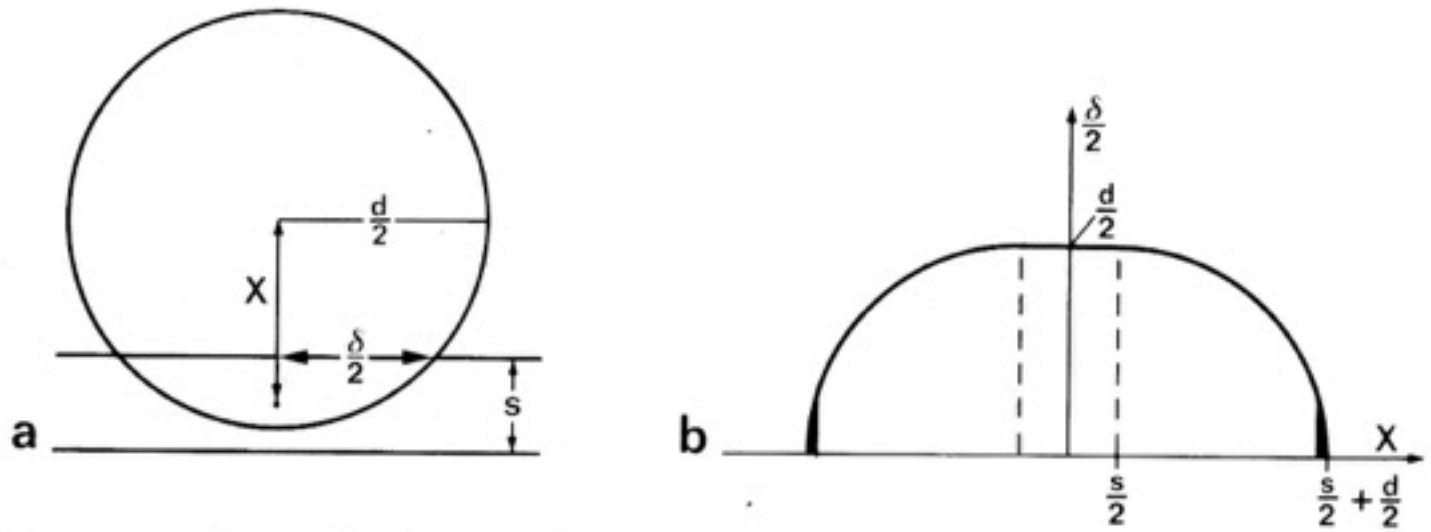

Fig. 7. **a** A sphere with diameter d is partly contained in a slice of thickness s. x is the distance between the center of the sphere and the middle layer of the slice. δ is the diameter of the part contained in the slice. **b** Dependence of δ on x. This is the distribution of apparent diameters δ if all the positions of particles of uniform size relative to a histological section occur with equal probability.

$$\bar{\delta} = \frac{ds + \pi d^2/4}{s + d}$$

$$d = \frac{2}{\pi}\left(\bar{d} - t + \sqrt{(\bar{d} - t)^2 + \pi \bar{d} t}\right)$$

$$d = \frac{2}{\pi}\left(\bar{d} - t + \sqrt{(\bar{d} - t)^2 + \pi \bar{d} t - v\pi^2/4}\right)$$

$\bar{d}$ = measured average diameter
d = real average diameter
t = thickness of section
v = variance

From Schüz and Palm (1989)

$\approx 9 \times 10^4$ neurons/mm^3

2) Counting synapses

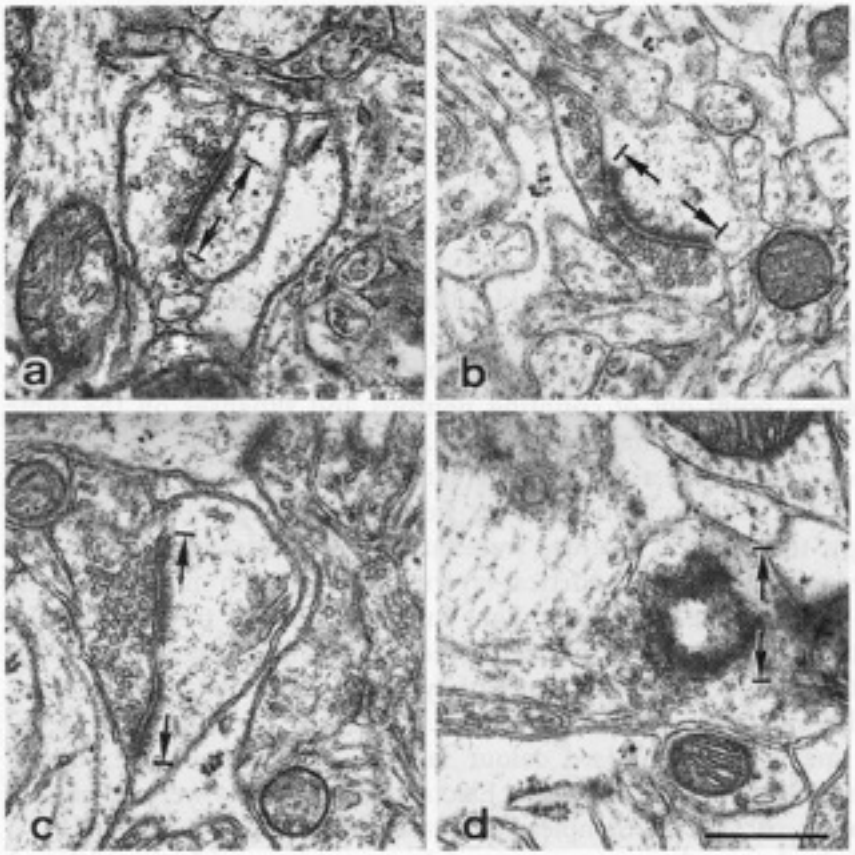

Fig. 13 a–d. Some examples of synapses on electron micrographs, to show how their size was measured between the lines marked by arrows. Synapse **a** is straight, **b** is curved, **c** has an interrupted postsynaptic thickening and **d** is cut tangentially. The *bar* at **d** is 0.5 µm long. (Schüz and Palm, 1989)

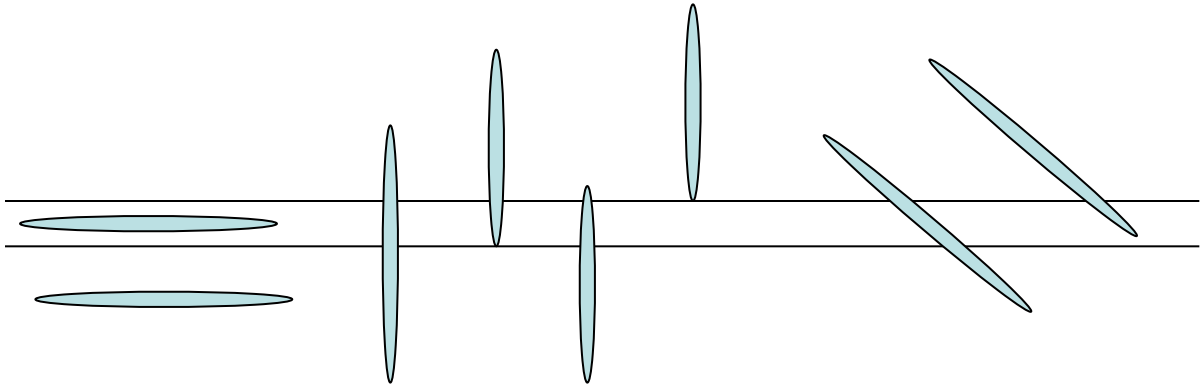

Section thickness ~ 60 nm

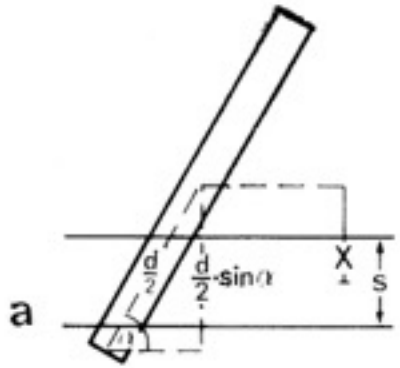
a
X
s
$\frac{d}{2}\cdot\sin\alpha$

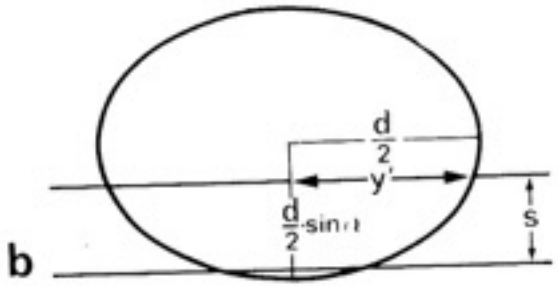
b
$\frac{d}{2}$
y'
$\frac{d}{2}\cdot\sin\alpha$
s

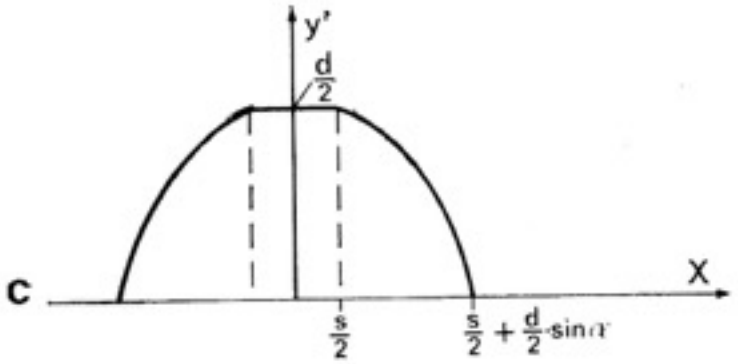
c
y'
$\frac{d}{2}$
X
$\frac{s}{2}$
$\frac{s}{2}+\frac{d}{2}\cdot\sin\alpha$

$$d = \frac{1}{2}\left(\bar{d} - \frac{4}{\pi}t + \sqrt{\left(\bar{d} - \frac{4}{\pi}t\right)^2 + 4\bar{d}t}\right)$$

$$d = \frac{1}{2}\left(\bar{d} - \frac{4}{\pi}t + \sqrt{\left(\bar{d} - \frac{4}{\pi}t\right)^2 + 4\bar{d}t - v}\right)$$

From Schüz and Palm (1989)

$\approx 7 \times 10^8$ synapses/mm^3

THE JOURNAL OF COMPARATIVE NEUROLOGY 231:175–179 (1985)

An Empirical Assessment of Stereological Formulae Applied to the Counting of Synaptic Disks in the Cerebral Cortex

MARC COLONNIER AND CLERMONT BEAULIEU
Départment d'Anatomie et Laboratoires de Neurobiologie, Faculté de Médecine, Université Laval, Québec, G1K 7P4 Canada

TABLE 3. Estimated Numbers of Test Objects Using Different Formulae[1]

	Original no.	$\frac{N_A}{\bar{d}}$	$\frac{8N_A\bar{Z}}{\pi^2}$	$\frac{N_A}{\bar{d}\times 4/\pi+t}$	Anker and Cragg
Polydispersed					
Circular					
Carrot slices	182				
Tangerine rinds	88				
Grapefruit rinds	37				
Oval					
Carrot slices	150				
Monodispersed					
Circular					
Carrot slices	150				

[1] $\bar{d}$, mean trace length of profiles of test objects; $\bar{Z}$, mean of the reciprocals of the trace lengths; N_A, number of profile per unit area.

From Colonnier and Beaulieu (1985)

TABLE 3. Estimated Numbers of Test Objects Using Different Formulae[1]

	Original no.	$\frac{N_A}{\bar{d}}$	$\frac{8N_A\bar{Z}}{\pi^2}$	$\frac{N_A}{\bar{d}\times 4/\pi+t}$	Anker and Cragg
Polydispersed					
Circular					
Carrot slices	182	181 (−0.5%)	191 (+5%)	123 (−32%)	131 (−28%)
Tangerine rinds	88	82 (−7%)	119 (+35%)	68 (−23%)	44 (−50%)
Grapefruit rinds	37	38 (+2%)	42 (+13%)	32 (−14%)	29 (−21%)
Oval					
Carrot slices	150	154 (+3%)	151 (+.7%)	102 (−32%)	112 (−25%)
Monodispersed					
Circular					
Carrot slices	150	178 (+19%)	166 (+11%)	117 (−22%)	117 (−22%)

[1] $\bar{d}$, mean trace length of profiles of test objects; $\bar{Z}$, mean of the reciprocals of the trace lengths; N_A, number of profile per unit area.

From Colonnier and Beaulieu (1985)

Disector method (Sterio 1984; Gundersen)

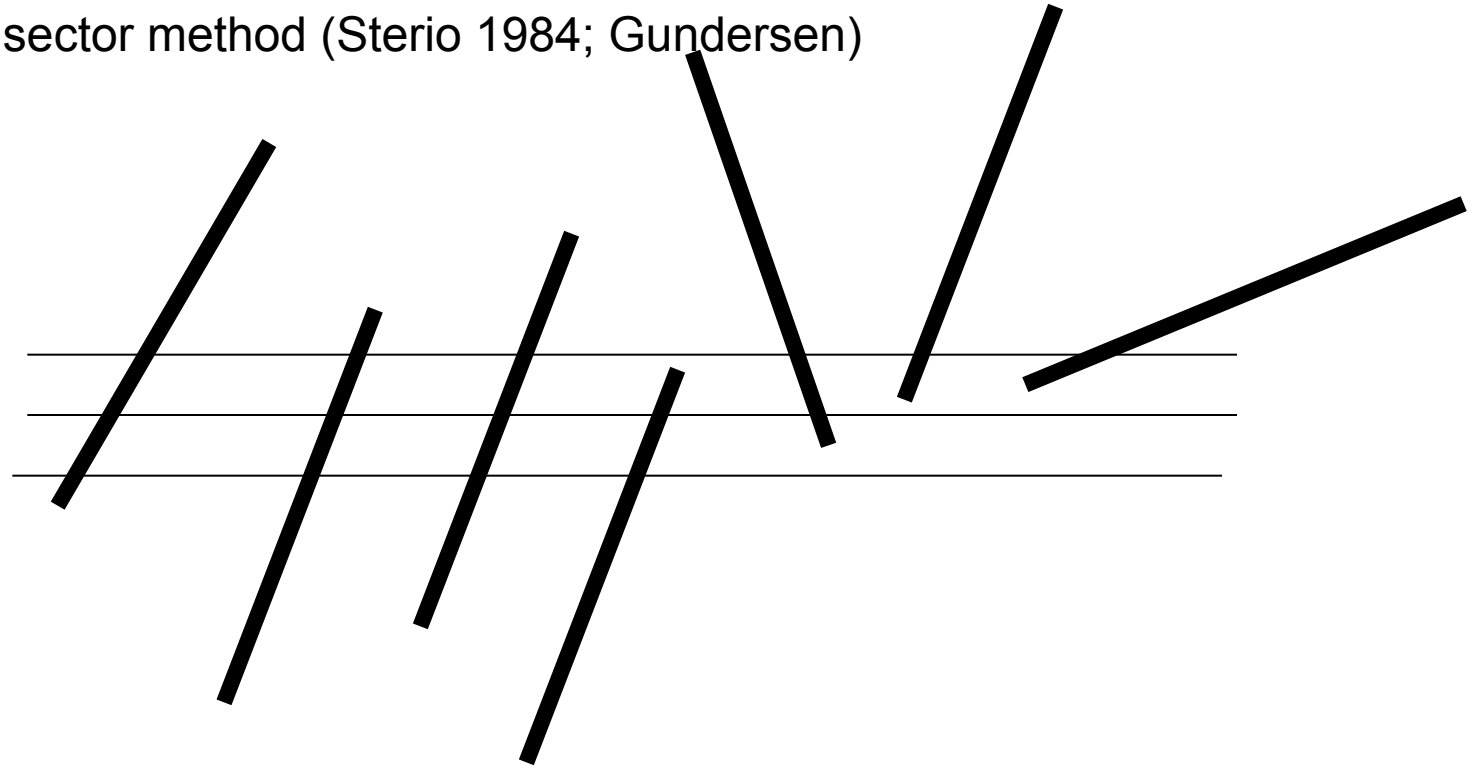

1) Counting cell bodies

2) Counting synapses

3) Length of dendrites or axons per neuron

4) Density of axons per mm^3

5) Density of spines per dendritic length

6) Density of synapses along dendrites

7) Density of synapses along axons

7) Probability of connections between neurons

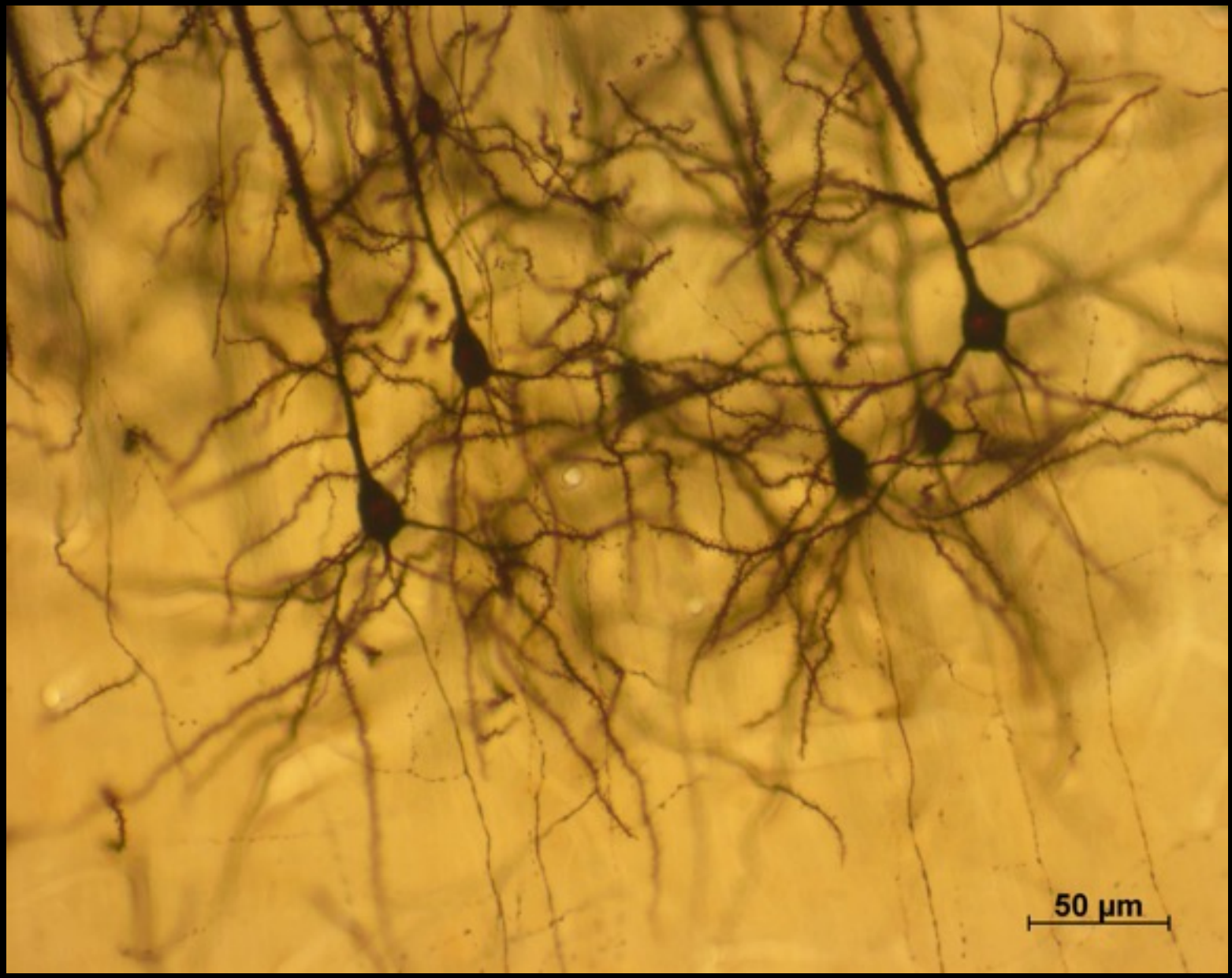

Golgi Macaca mulatta

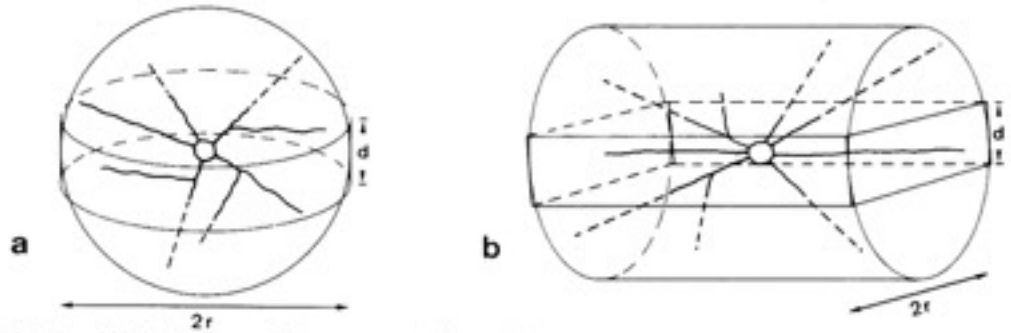

Fig. 32 a, b. To illustrate the way we inferred the size of the dendritic or axonal tree of a neuron from the part measured in a histological section of thickness *d*. Spherical symmetry of the ramification is assumed in **a** and cylindrical symmetry in **b**. *r* is the radius of the sphere or cylinder, equal to the longest fibre measured in the preparation

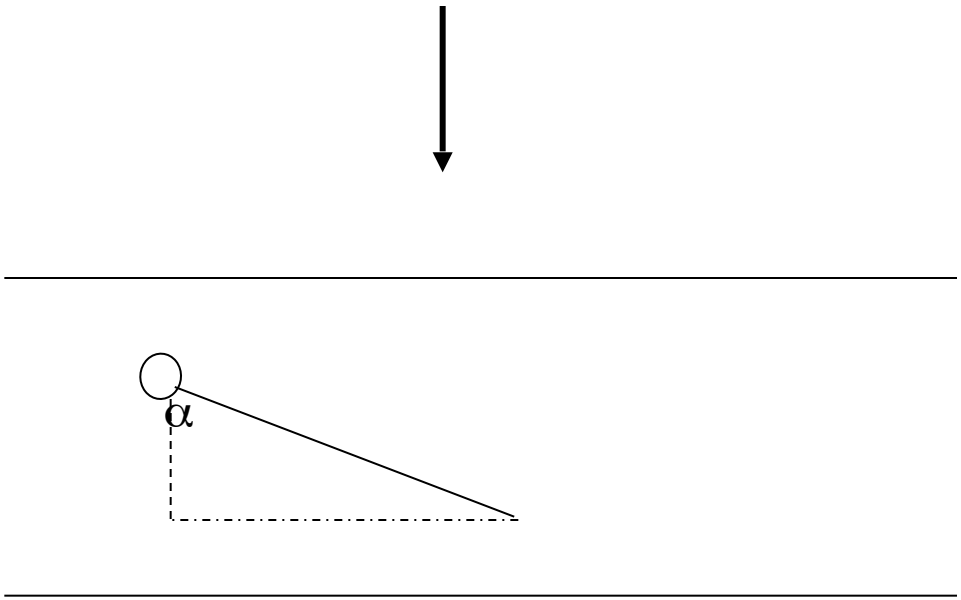

Shortening of the lengths due to projection:

$$\frac{1}{\pi/2}\int_0^{\pi/2} \sin\alpha \, d\alpha = \frac{2}{\pi} .$$

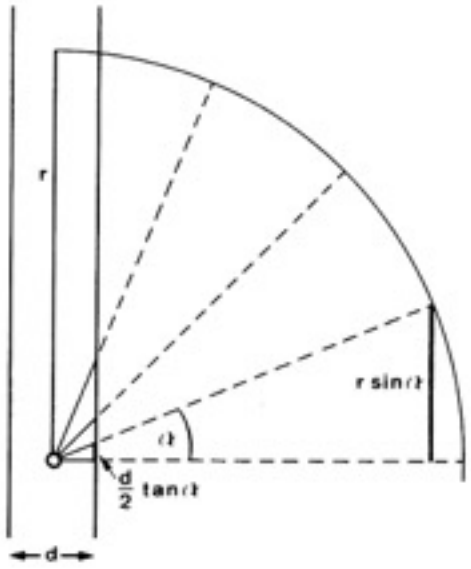

Fig. 33.
Fibres of equal length r emanating from a neuron located in the middle of a slice of thickness d. The drawing illustrates how the length of all the fibres of that neuron can be calculated from the projections of the cut fibres. For explanation see text ("correction III")

$$2 \cdot r/d \qquad \text{(correction III)}$$
$$\pi/2 \cdot 4/3 \cdot r/d = 2.09 \cdot r/d \qquad \text{(correction I combined with IIa)}$$
$$\pi/2 \cdot \pi/2 \cdot r/d = 2.46 \cdot r/d \qquad \text{(correction I combined with IIb),}$$

$$2 \cdot r/d \qquad \text{(correction III)}$$
$$\pi/2 \cdot 4/3 \cdot r/d = 2.09 \cdot r/d \qquad \text{(correction I combined with IIa)}$$
$$\pi/2 \cdot \pi/2 \cdot r/d = 2.46 \cdot r/d \qquad \text{(correction I combined with IIb),}$$

≈ 10 – 40 mm axon/neuron

1) Counting cell bodies

2) Counting synapses

3) Length of dendrites or axons per neuron

4) Density of axons per mm^3

5) Density of spines per dendritic length

6) Density of synapses along dendrites

7) Probability of connections between neurons

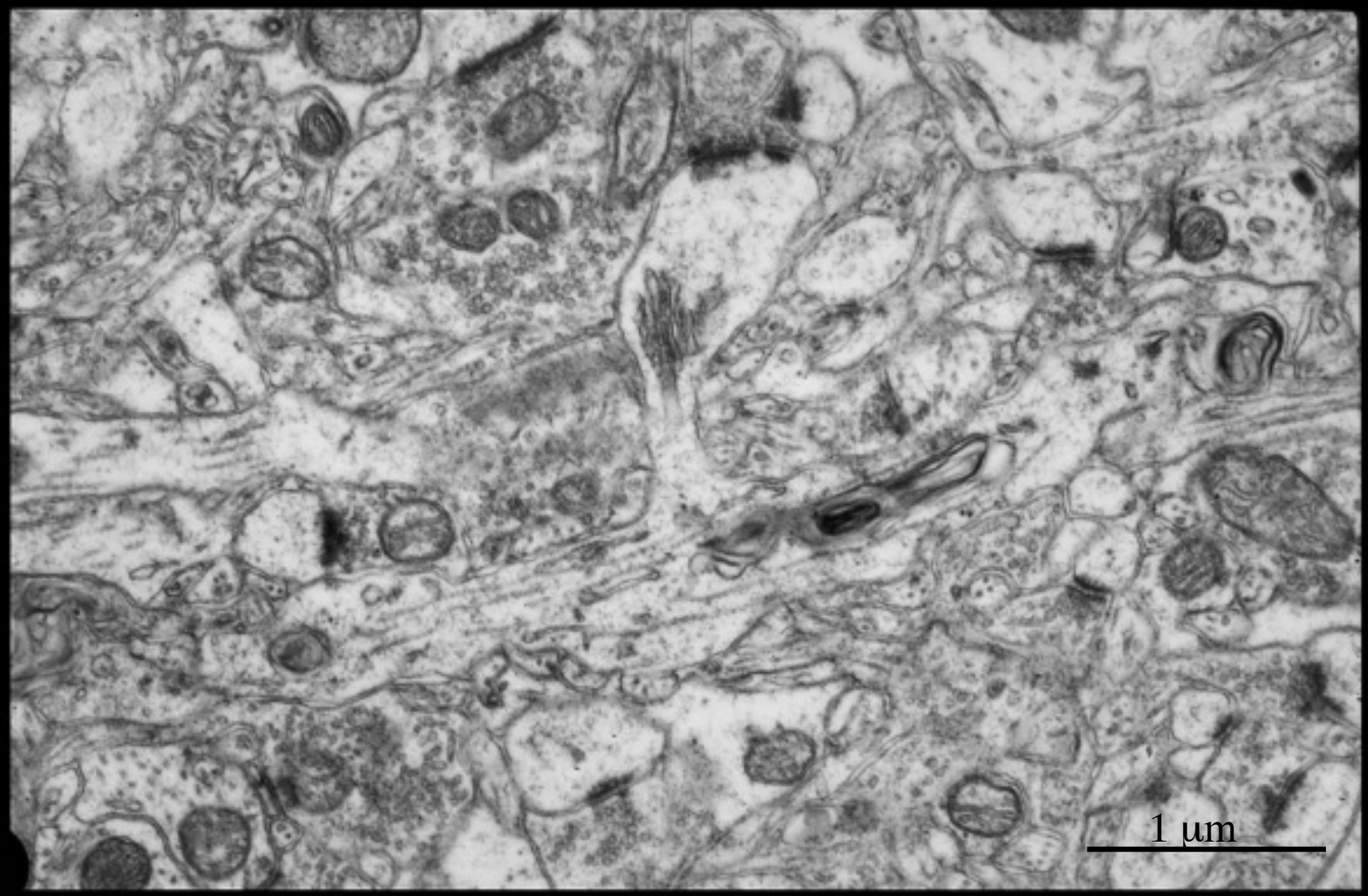
1 µm

Dendrites	35 %
Axons	34 %
Spines	14 %
Glia processes	11 %
Extracellular space	6 %

		Neve cell bodies	11 %
		Glia cell bodies	1 %
		Blood vessels	4 %
Dendrites	35 %		29 %
Axons	34 %		29 %
Spines	14 %		12 %
Glia processes	11 %		9 %
Extracellular space	6 %		5 %

		Neve cell bodies	11 %
		Glia cell bodies	1 %
		Blood vessels	4 %
Dendrites	35 %		29 %
Axons	34 %		29 %
Spines	14 %		12 %
Glia processes	11 %		9 %
Extracellular space	6 %		5 %

≈ 1 - 4 km axon/mm^3

1) Counting cell bodies

2) Counting synapses

3) Length of dendrites or axons per neuron

4) Density of axons per mm^3

5) Density of spines per dendritic length

6) Density of synapses along dendrites

7) Density of synapses along axons

8) Probability of connections between neurons

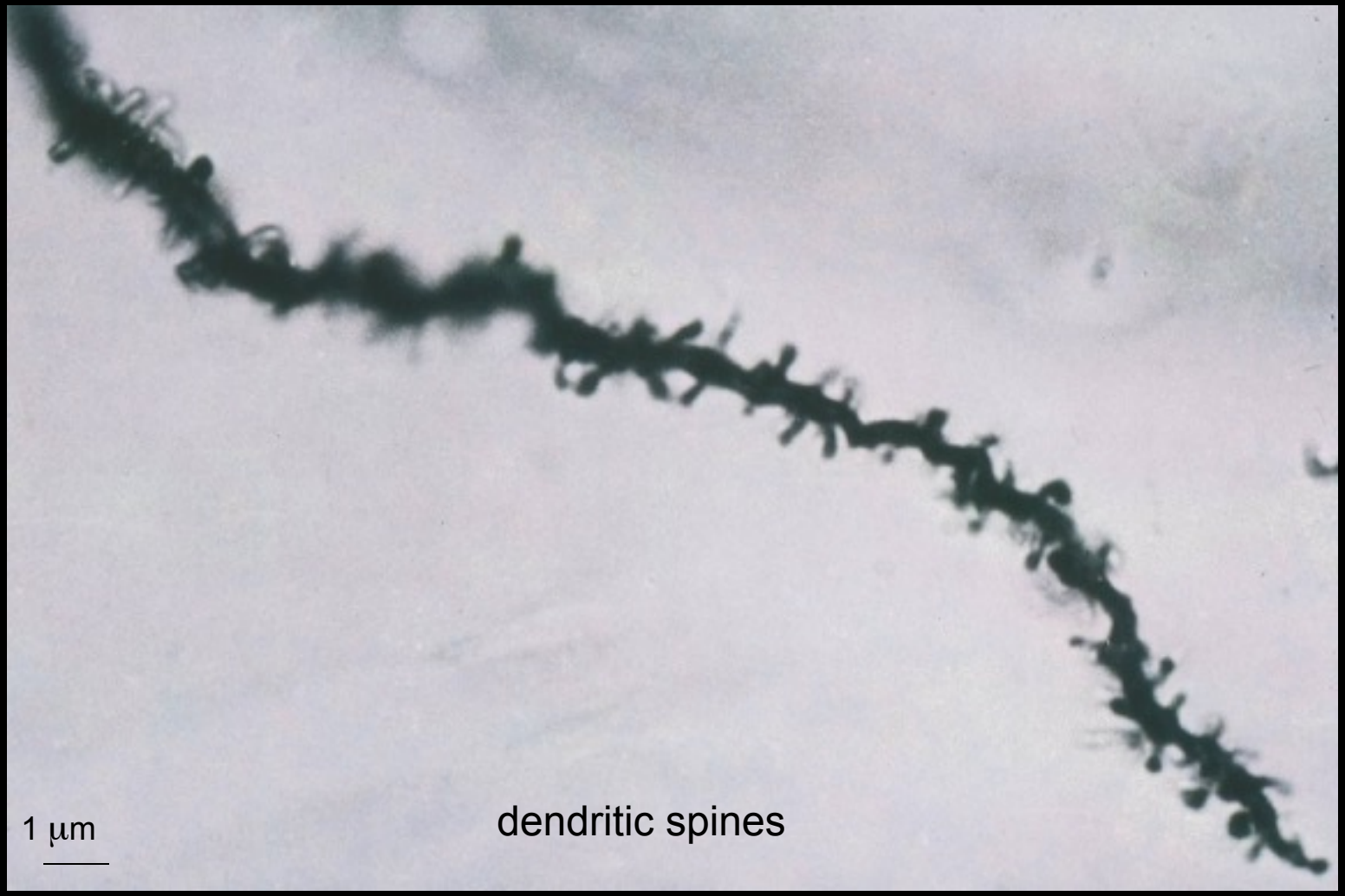

dendritic spines

Fig. 1. Segment of 29 μm of an apical dendrite drawn with the Camera lucida ($\times$ 3,000). The points indicate the tips of the spines. In the two regions between the long vertical lines their average projected distance from the axis of the dendrite was measured and the average radius of the dendrite subtracted. The average radius and the number of spines were taken from the whole segment. (For the purpose of this illustration the drawing was reduced to a magnification of $\times$ 2,000.)

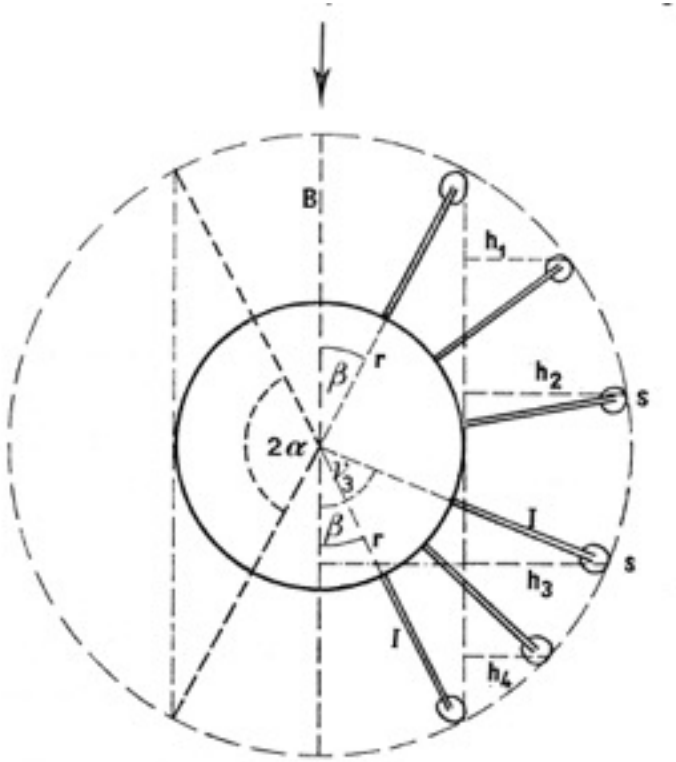

Fig. 2. Scheme of the cross section of a dendrite (circle in the middle) with some spines s. The observer looks in the direction of the arrow. B: optical axis of the microscope; h_{1-4}: lengths of four spines projected onto the visual plane; l, real length of the spines; r, radius of the dendrite; α, angle which subtends one fourth of the spines visible in the microscope; β, angle which subtends one fourth of the spines hidden by the dendrite; γ_3, angle of a spine with the optical axis.

Fig. 1. Segment of 29 μm of an apical dendrite drawn with the Camera lucida ($\times$ 3,000). The points indicate the tips of the spines. In the two regions between the long vertical lines their average projected distance from the axis of the dendrite was measured and the average radius of the dendrite subtracted. The average radius and the number of spines were taken from the whole segment. (For the purpose of this illustration the drawing was reduced to a magnification of $\times$ 2,000.)

≈ 1 spine/1-2 µm

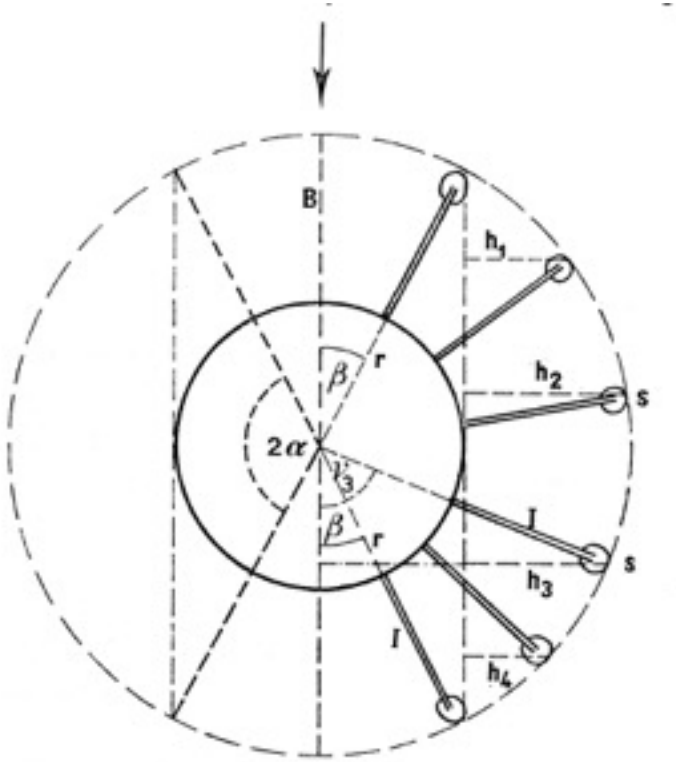

Fig. 2. Scheme of the cross section of a dendrite (circle in the middle) with some spines s. The observer looks in the direction of the arrow. B: optical axis of the microscope; h_{1-4}: lengths of four spines projected onto the visual plane; l, real length of the spines; r, radius of the dendrite; α, angle which subtends one fourth of the spines visible in the microscope; β, angle which subtends one fourth of the spines hidden by the dendrite; γ_3, angle of a spine with the optical axis.

Density of synapses along dendrites

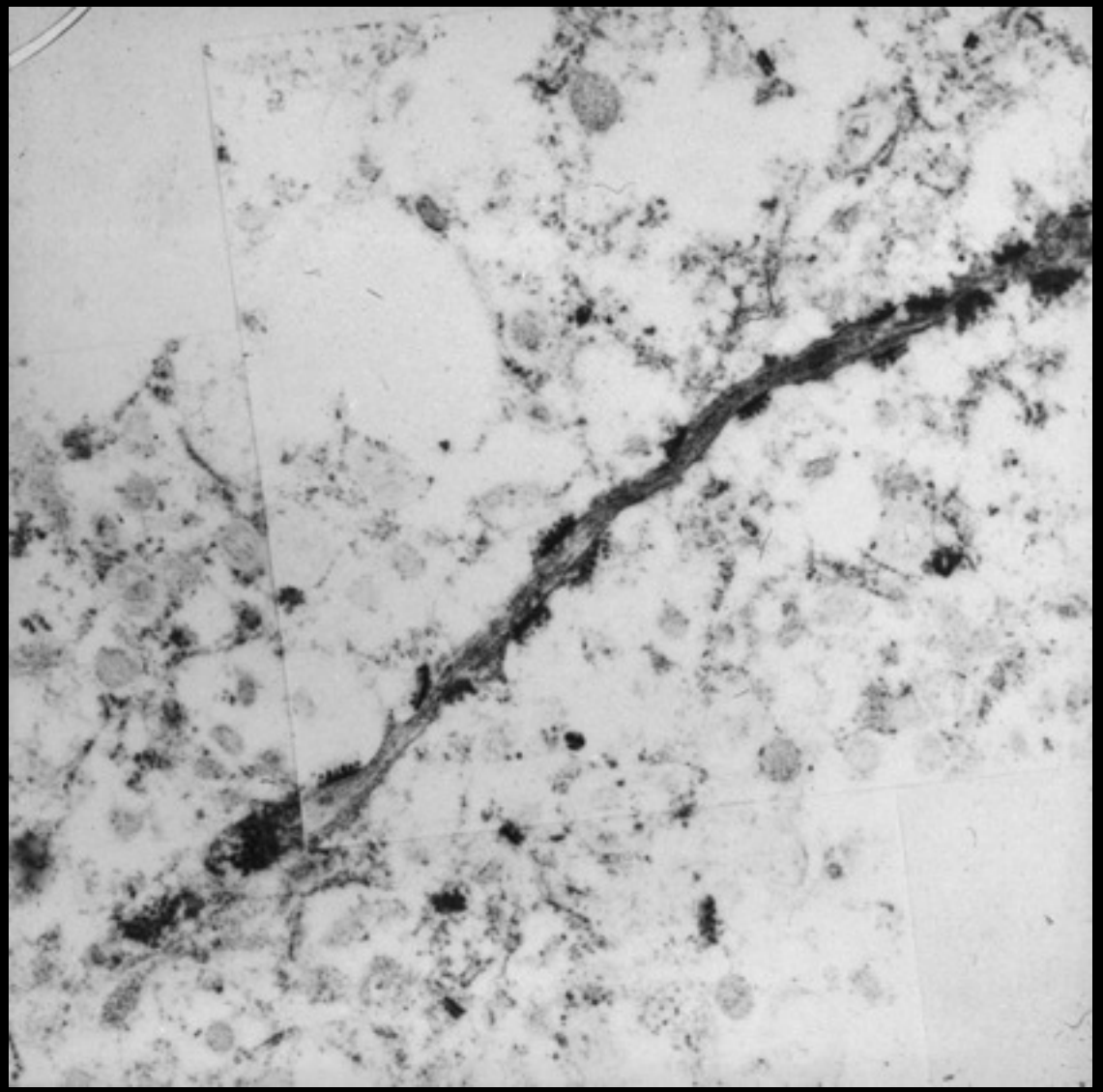

≈ 3 synapes/µm

1) Counting cell bodies

2) Counting synapses

3) Length of dendrites or axons per neuron

4) Density of axons per mm^3

5) Density of spines per dendritic length

6) Density of synapses along dendrites

7) Density of synapses along axons

8) Probability of connections between neurons